Structure-Based Virtual Screening, Molecular Docking, MolecularDynamics Simulation of VEGF Inhibitors for the Clinical Treatment of Ovarian Cancer

Sourav Mukherjee
Eminent Biosceinces
Mohnad Abdalla
Shandong University Cheeloo College of Medicine
Manasi Yadav
Eminent Biosciences
Maddala Madhavi
Department of Zoology, Osmania University
Ravina Khandelwal
Eminent Biosciences
Leena Prajapati
Eminent Biosciences
Aravind Panicker
Eminent Biosciences
Aashish Chaudhary
Eminent Biosciences
Ashraf Al-Brakati
Taif University
Tajamul Hussain
King Saud University
Anuraj Nayarisseri (anuraj@eminentbio.com)
Alagappa University
Sanjeev Kumar Singh
Alagappa University

Research Article

Keywords: Ovarian Cancer, VEGF, VEGF inhibitors, Molecular Docking, Virtual Screening, Molecular Dynamics, ADMET studies, Egg Plot.

Posted Date: October 15th, 2021

DOI: https://doi.org/10.21203/rs.3.rs-840860/v1

Abstract

VEGF and its receptor play an important role both in physiologic and pathologic angiogenesis, which is identified in ovarian cancer progression and metastasis development. The aim of the present investigation is to identify a potential VEGF inhibitor which is playing a crucial role in stimulating the immunosuppressive microenvironment in tumour cells of ovary and to examine for an effectiveness of identified inhibitor for treatment of ovarian cancer using various In silico approaches. 12 established VEGF inhibitors were collected from various literature. The compound AEE788 displays the great affinity towards the target protein as a result of docking study. AEE78 was further used for structure base virtual screening in order to obtain more structurally similar compound with high affinity. Among the 80 Virtual screened compounds, CID 88265020, explicates much better affinity than established compound AEE788. Based on Molecular Dynamics Simulation, pharmacophore and comparative toxicity analysis of both the best established compound and the best virtual screened compound displayed a trivial variation in associated properties. The virtual screened compound CID 88265020 have the high affinity with the lowest re-rank score, and holds a huge potential to inhibit the VGFR and can be implemented for prospective of future investigations in Ovarian Cancer.

1. Introduction

Ovarian cancer is the most lethal gynaecologic malignancy and it is a type of disease in which malignant (cancer) cells form in the tissue coating the ovary. Ovarian cancer is the seventh most frequent cancer among women and among other cancers ovarian cancer is one among the top ten regular reason of death from cancer throughout globe[1]. The prediction stated that due to ovarian cancer there were > 120,000 deaths worldwide in every year [2]. Statistically half of all ovarian cancers are begin in women of an age of 65 years or greater and for this reason, limited survivability possibility for women [1]. Maximum ovarian cancers develop after menopause. Women who have ovulated more over their lifetime are at an extended risk of ovarian cancer. Some combination of surgery, radiation therapy, and chemotherapy during the primary stage of ovarian cancer exhibits the overall five-year survival rate in the Western countries is around 35–45% [3]. Ovarian carcinoma is the most frequent type of ovarian cancer. Five chief subtypes are there in ovarian carcinoma in which high-grade serous carcinoma is the most typical type and germ cell tumors, sex cord-stromal tumors are the less typical types of ovarian cancer. The initial mutation in BRCA1 and BRCA2, DNA mismatch genes lead to ovarian cancer [3]. The risk of ovarian cancer rises in those women who possess a family history of ovarian cancer [3]. BRCA mutations are associated with high-grade serious non mucinous epithelial ovarian cancer whereas Lynch syndrome is initiated by mutations in mismatch repair genes[3]. Therefore there is an extreme necessity to identify newer inhibitors and drugs for the betterment of survival in ovarian cancer. Vascular Endothelial Growth Factor A (VEGF A) which was formally identified as VEGF, is an essential regulator of angiogenesis in both normal tissues and in tumors [4].VEGF A is also crucial for provoking the immunosuppressive microenvironment in tumors[5].VEGF further enhances cell survival, proliferation, and migration. Investigations have disclosed that VEGF is over expressed by ovarian cancer. The expression of VEGF

and IL-8 in ovarian cancer are following the transcriptional regulation of nuclear factor kappaB (NF-kB)[6]. VEGFR 1(Flt-1) and VEGFR2(Flk-1) are the two most important member of the VEGFR family which plays a significant role in angiogenesis[7]. VEGFR 2 reconciles the angiogenic and permeability-enhancing effect of VEGF while VEGFR 1 performs a role in angiogenesis by selecting bone marrow-derived cells and monocytes into the tumor vasculature[7].Bevacizumab is a recombinant monoclonal antibody that inhibits the VEGF signalling pathway by binding to circulating VEGF A and have been widely appraised in ovarian cancer treatment[8].Still, various inhibitor investigations are progressing on to direct antagonistic against VEGF and its mechanisms, including different signalling pathways. The present study concentrates on drug discovery which exhibits inhibitory impacts on VEGF protein and therefore, ascents apoptosis of ovarian cancer.

2. Results

2.1 Protein and ligand preparation

The signaling protein, Vascular Endothelial Growth Factor Receptor 2 (VEGFR-2 PDB ID: 3V2A), obtained from protein database bank, was cleaned using Schrödinger module before visualization of its X-ray diffraction data with RasMol software; depicted in ribbon and backbone model [Fig. 1]. The target protein has two chains with 280 groups of 2114 atoms and total 2160 bonds. There are three spring-shaped alpha-helices in red-color, and 25 beta-strands in blue color, however no turns and loops. The binding of ligand could be anticipated from protein-folds of the target VEGF protein. Before docking, ligand preparation was done in the LigPrep module of Schrodinger suite, 2013.

2.2 Molecular Docking

The docking results of the 12 established compounds in the first cavity which is the largest cavity of the target protein VEGF listed in Table 1. Among all the established compounds[Table 7], AEE788 (PubChem ID 10297043) is resulted as the best-established compounds as it shows the lowest re-rank score among all compounds and has the highest affinity towards the VEGF. The compound also has high-affinity and physicochemical properties such as molecular weight 440.595 g/mol, hydrogen bond donor counts 2 and hydrogen bond acceptor count 5, and logP value of 4.6. The compound holds a re-rank score-95.9802 with the H-bond interaction score of -2.5. Hence, this compound was identified as the best- established compound against the target protein VEGF.

Table 1
Established compounds docking study result.

Ligand	Filename	MolDock Score	Rerank Score	HBond	MW
10297043	[02]10297043	-121.765	-95.9802	-2.5	440.583
123631	[00]123631	-116.826	-91.3569	-1.27851	446.902
9933475	[01]9933475	-121.08	-90.3479	-2.26465	450.505
216239	[04]216239	-106.066	-90.2369	-4.5783	464.825
9809715	[03]9809715	-130.606	-88.876	-1.88135	539.625
123631	[01]123631	-106.039	-87.1955	-1.95681	446.902
9911830	[00]9911830	-120.891	-86.9845	-8.73156	454.863
9911830	[03]9911830	-116.349	-85.2625	-1.99962	454.863
9911830	[01]9911830	-116.111	-84.7526	-1.6096	454.863
10297043	[04]10297043	-114.998	-84.607	0	440.583
10113978	[00]10113978	-110.567	-84.4218	-2.45945	437.518
9933475	[02]9933475	-112.536	-84.2488	-2.42747	450.505

2.3 Virtual screening

Similarity search of the best-established compound against PubChem database resulted in 80 compound structures that gave a = > 95 similarity percentage. Table 2 records the top 11 compounds that exhibit the greatest affinity to the target protein VEGF. The compound with PubChem ID 88265020 was recognized to hold the lowest re-rank score and was therefore confirmed as a compound with the greatest affinity towards the targeted protein. Some of the physical properties of the virtual screened compound comprise of molecular weight of 569.783g/mol, hydrogen bond donor count of 5, hydrogen bond acceptor count of 7 and a logP value of 6.1. The re-rank score of this compound attains at -112.171 and the H-bond interaction score is -8.6315. Therefore, between a total of 80 compounds, the compound PubChemID-88265020 possess a much greater ability to inhibit the target protein VEGF against ovarian cancer subjected to further analysis.

Table 2
Docking study result for virtual screened compounds with reference to high-affinity Virtual screened compounds with reference to high affinity established compound AEE788 (PubChem ID 10297043)

Ligand	Filename	MolDock Score	Rerank Score	HBond	MW
88265020	[00]88265020	-149.521	-112.171	-8.6315	569.783
88265020	[01]88265020	-149.487	-109.471	-1.81064	569.783
88265020	[04]88265020	-128.011	-101.733	-3.45831	569.783
71313049	[00]71313049	-125.348	-100.642	-7.07561	440.583
44629455	[00]44629455	-131.699	-99.8896	-2.5	442.599
10297042	[03]10297042	-128.873	-99.1998	-0.10172	440.583
69170098	[04]69170098	-122.43	-98.656	-2.5	412.53
69232929	[00]69232929	-125.312	-98.3018	-7.16336	412.53
16071547	[01]16071547	-128.745	-97.5661	-3.87498	516.679
16071547	[03]16071547	-118.562	-96.8667	0	516.679
69232929	[01]69232929	-127.435	-96.8654	-4.88497	412.53

2.4 Molecular Dynamics Simulation

The dynamic simulation of a molecule provides details of probable conformational changes over a trajectory, comparable to biological environment. The simulation result is analyzed over structural analysis by RMSD and RMSF, ligand properties, and protein-ligand interaction. The root mean square deviation (RMSD) graph suggests structural stability of protein-ligand interaction, lower RMSD confers greater stability. Root mean square fluctuation (RMSF) graph indicates mobility of protein residue. The inter-residue interaction for established compounds shows to be more stable compared to virtually screened compounds. The protein RMSD for AEE788 is in between 3.0 to 4.2 Å with deviation around 20ns, and the ligand graph follows the estimated trend as protein except for deviation between 40-60ns. [Fig. 2**(I)**]. This suggests the protein-ligand interaction is steadier; confirmed with the RMSF graph for AEE788 ranged 1–8 Å, where peaks are more frequent implying more flexible amino acids are on protein's C backbone. [Fig. 2 **(II)**]. The RMSD graph for protein-lead compounds is more volatile comparatively. The protein RMSD fluctuates from 2.4 to 6.5 Å at frequent intervals and lead compound RMSD spans over 2.5 to 22.5Å with recurrent variation over the trajectory. [Fig. 2**(III)**]. It is noted that mean value of protein-ligand interaction for virtually screened compounds is more than AEE788, hence less stable. Beside there are fewer peaks in the RMSF graph which alludes less flexibility in protein's C backbone. [Fig. 2**(IV**)].

2.4.2 Protein-Ligand interaction

Molecular dynamic simulation gives insight into probable protein-ligand interaction for established compound and virtually screened compound, depicted with histogram and heatmap [Fig. 3] [Fig. 4]. The interface between protein and ligand comprises four types of bonds: hydrogen bonds, hydrophobic interaction, ionic bonds, and water bridges; hydrogen bond plays significant role in ligand binding and drug specificity.The histogram for protein-established compound propones its hydrophobic nature which means pi-cation, pi-pi, and other nonspecific interactions are present [Fig. 3 **(C)**]. The amino acid residues PRO_49, MET_78, MET_81, HIS_133, MET_197 and ILE_215 exhibits more hydrophobic interaction, of these, HIS_133 showed strongest interaction [Fig. 3**(A)**], as confirmed by heatmap [Fig. 3**(B)**]. The hydrogen bonding which strongly influences drug specificity, metabolization and adsorption is by few residues LYS_48, GLN_79 and TYR_165, alongside, only GLU_30 residue shows ionic interaction inferring the established compound is not much ligand specific. However, some residues GLU_30, LYS_48, SER_50, CYS_51, PRO_53, THR_77, GLN_79, ARG_164, TYR_165, GLY_196 are forming water bridges (hydrogen bonded protein-ligand interaction mediated by water molecules). The [Fig. 3**(B)**] is a heatmap for individual residue interaction with protein over a trajectory frame, the intensity of color enumerates interactions of amino acids.

The protein-lead compound interaction, depicted in [Fig. 4] suggest overwhelming hydrophobic interaction and water bridges. This compound shows more hydrogen bonding, owing to hydroxylamine octyl chain. TYR_165 asserts strongest hydrophobic interaction along with PRO_166, TYR_194, MET_197, PHE_199 residues [Fig. 4**(A)**]. This interaction is by strong pi-pi bonding of residue with aromatic ring [Fig. 4**(C)**], while other hydrophobic interaction is quite less strong. The virtually screened compound is showing ionic bond by residue GLU_167, plausibly with additional hydroxylamine functional group. And residues like MET_213 and GLN_132 are forming hydrogen bond by back donating [Fig. 7]. The water bridges are formed by residues TYR_165, GLU_167, TYR_194, GLN_210. Which also connote this surface is exposed for binding.The heatmap for this interaction insinuate only few residues like TYR_165, PRO_166, GLU_167, TYR_194, MET_197, and PHE_199 have a greater number of contacts over trajectory frame compared to others. The number of specific contacts made by protein with ligand vary from zero to nine [Fig. 4**(B)**].

2.4.3 Ligand property

The ligand property was analyzed over a range of parameters: root-mean square deviation (RMSD), radius of gyration (rGyr), molecular surface area (MolSA), solvent accessible surface area (SASA), and polar surface area (PSA), giving structural details.The RMSD graph demonstrating stability of the compound, for established compounds is ranged from 1–3 Å with minimal fluctuation and mean near 2 Å. The radius of gyration is the distance of an atom from the center of mass of the molecule, in order to obtain the same moment of inertia; it provides insight into the overall dimension of the protein. The rGyr value is in between 4.8-6 Å with mean at 5.2 Å. The molecular surface area is calculated using 1.4 probe

radius; it gives insight on Van Der Waals surface area. The MolSA is ranged between 424–448 $Å^2$ with minimal fluctuation around 80 ns. The solvent surface area is a water accessible area which ranges from 200 to 500 $Å^2$ and is highly variable with two equilibrium peaks around 300 $Å^2$ and 400 $Å^2$. The polar surface area is surface accessible for binding of ionic molecules. The PSA value was stable over the trajectory with mean at 80 $Å^2$. [Fig.5]

The virtual screened compound's RMSD trajectory is erratic range from 1–4 Å with fluctuation between 20 to 80 ns. The rGyr is stable between 20 to 60 ns and 80–100 ns, ranging between 6.4 to 8.8 Å, which is higher than the established compound. The molecular surface area ranged from 580 to 600 $Å^2$ with fluctuation around 50 ns and equilibrium approximately 595 $Å^2$ which is more compared to the established compound (432 $Å^2$). Also, the solvent accessible surface area is more erratic varying from 500 to 1000 $Å^2$ and mean polar surface area is 160 $Å^2$. As the surface area of virtual screened compounds is relatively more compared to established compounds, attributed to the octyl hydroxylamine chain, the mean value of surface areas and radius of gyration is also higher and it also gives more flexibility to ligands which could be seen from the RMSD graph. [Fig. 6**].** The ligand property of virtually screened compound (PubChem CID: 88265020) is studied more with pharmacophore mapping.

2.5 Drug - Drug Comparative study

Drug-drug Comparative study records the MolDock Scores and re-ranks scores of the best- established compound and the best virtual screened compound against the target protein VEGF on ovarian cancer [Table 3]. The table indicates that the best-virtual screened compound holding PubChem ID: 88265020 has a higher binding affinity to the target VEGF protein if correlated to the best- established compound AEE788 (PubChem ID: 10297043) due to a lower re-rank score counts − 112.158. The compound holding PubChem ID 88265020 discloses lower MolDock Scores and re-rank scores for several additional essential characteristics like External ligand interactions, protein-ligand interactions, hydrogen bonds which intimates that this compound occupies a greater affinity to the VEGF protein. A steric value measured by PLP (Piecewise Linear Potential) is lower for the best virtual screened compound whereas, in the case of LJ12-6(Leonard-Jones approximation) method, it shows lower value for the best-established compound. Therefore, it illustrates that both the compounds have comparable possible inhibition against the VEGF protein.

Table 3
Drug-Drug comparative study

	Established Compound PubChem ID: 10297043		**Virtual Screened Compound (PubChem ID: 88265020)**	
Energy overview: Descriptors	MolDock Score	Rerank Score	MolDock Score	Rerank Score
Total Energy	-121.763	-95.967	-149.505	-112.158
External Ligand interactions	-143.736	-122.464	-174.491	-144.108
Protein - Ligand interactions	-143.736	-122.464	-174.491	-144.108
Steric (by PLP)	-141.236	-96.888	-165.861	-113.781
Steric (by LJ12-6)		-23.596		-23.493
Hydrogen bonds	-2.5	-1.98	-8.63	-6.835
Hydrogen bonds (no directionality)		0		0
Electrostatic (short range)	0	0	0	0
Electrostatic (long range)	0	0	0	0
Cofactor - Ligand	0	0	0	0
Steric (by PLP)	0		0	
Steric (by LJ12-6)		0		0
Hydrogen bonds	0	0	0	0
Electrostatic	0	0	0	0
Water - Ligand interactions	0	0	0	0
Internal Ligand interactions	21.973	26.497	24.986	31.95
Torsional strain	7.658	7.183	16.15	15.148
Torsional strain (sp2-sp2)		3.952		3.436
Hydrogen bonds		0		0
Steric (by PLP)	14.315	2.462	8.836	1.52
Steric (by LJ12-6)		12.9		11.845
Electrostatic	0	0	0	0
Soft Constraint Penalty	0		0	
Search Space Penalty	0		0	

2.6 Pharmacophore mapping

Pharmacophore mapping provides the quintessentialsystemic spatial feature of the molecular interaction of the ligand with the target receptor, apart from the method of molecular docking, for understanding the interactive characterization and provide a factual query on the suitable target interface. It imitates the aligned poses of the molecule and identifies the apt interaction between the target protein and the lead compound. Owing to this admirable affinity and good interaction profile of the virtually screened compound (PubChem ID 88265020), the study was conducted to obtain various kinds of analyzed pharmacophore interactions. The desired compounds were in .sdfformat for pharmacophore studies. The residue interaction of the best virtually screened compound (PubChem ID 88265020) in the cavity of VEGF protein was studied.

The Van Der Waals coupling of the VEGF protein structure and the virtually screened compound (PubChem ID 88265020) is displayed in [Fig. 7]. The electrostatic interaction is shown by Gly196, Met197, His133, Tyr194, Tyr165, Lys48, Met213 and Gln132 residues, symbolically encircled in pink, these residues are also involved in hydrogen bonding; whereas Pro49, Ala195, Pro166, Glu167, Ile215, and Ile212 residues are involved in van der Waals interactions, encircled in green. The residues represented with various shades and size blue halo around it infers the solvent-accessible surface of an interacting residue such as Tyr165 and Met213 residues: the size of halo is proportional to the accessible surface area.Furthermore, the solvent-accessible surface of an atom is represented by a blue halo around the atom and the diameter of the circle is proportional to the solvent-accessible surface. Met213, Gln132, and Tyr194 show the Hydrogen bond interactions with amino acid main chains are represented by a green dashed arrow directed towards the electron donor. Tyr165 with the compound shows pi-pi interaction is represented by an orange line with the pi symbol indicating the interaction.

The H-bond interactions of the virtual screened compound (PubChem ID: 88265020) having the lowest re-rank score possessing immense affinity at the active sites of the VEGF protein cavity [Fig. 8]. Hydrophilic and hydrophobic, electrostatic and H-bond interactions are the example of the pharmacophoric characteristics of the ligand-receptor interaction. Figure 8 represents the compound binding of the specific amino acid residues of the VEGF protein through a hydrogen bond. An amino acid Ile212, Met213, and Ala195 residue shows the four H-bond interactions represented by the blue dotted line [Fig. 8]. The virtual screened compound (Pubchem ID: 88265020) has the number of hydrogen bond interactions as compared to the established compound, AEE788 (PubChem ID 10297043).

The electrostatic interaction of virtual screened compound (PubChem ID-88265020) [Fig. 9] manifests that the clusters of charged and polar residues, that are detected on protein-protein interfaces, may intensify the stability of the complex; though the net effect of electrostatics is generally destabilizing. The virtually screened compound (PubChem ID-88265020) with VEGF protein having the high affinity was embedded in the protein cavity. The positive and negative areas of the protein are demonstrated by two types of variant colors: the red color evince the electro-negativity zone, whereas the electropositive zone

with blue color. The electrically neutral zone is shown with white colored surface. Most of the atoms of the target compound in the protein cavity were observed to be biased towards blue color zone inferring the high electro-positivity [Fig. 9].

Figure 10 represents the aromatic interactions with the most effective virtual screened compound (PubChem ID-88265020). The aromatic interaction is indicative of effective binding stability of the compound with protein. The aromatic conformation imparts an effect on the function of the complex molecule. The identified virtual screened compound (PubChem ID: 88265020) shows a higher affinity aromatic interaction in the VEGF protein binding site. In [Fig. 10], the blue color symbolizes the edges of the protein cavity with light shade surfaces and shade surfaces having color orange signifying the face. Here an amino acid His133, Met197, Gly196, Tyr165, Pro166, Ala195, Tyr194, Leu161, and Glu132 residues are showing aromatic interaction. These interactions coincide with molecular dynamic observation.

2.7 ADMET studies-Pharmacological and metabolic properties

AdmetSAR software was used to estimates various ADMET properties of the best-established compound AEE788 (PubChem ID 10297043) and the best virtual screened compound holding PubChem ID: 88265020 [Tables 4 & 5]. The SwissADME software briefing six essential properties of oral bioavailability is represented with bioavailability radar for best of the two best-established compounds and virtually-screened compounds [Fig. 11]; the pink region in radar is range of optimal value.

2.7.1 Absorption prediction of the compound

After the drug administration, ADMET blood-brain barrier model foretells the penetration of the drug across blood-brain barrier [Table 4]. The intestinal absorption of a drug is prognosticated by HIA after oral administration. While comparing with the established drug, ADMET absorption level of compound is revealing good absorption [Table 4]. A monolayer tissue culture of an ideal human colon adenocarcinoma (referred as, Caco-2) is acknowledged as a standard for testing drug permeability in drug discovery, the foretold effects exhibit permeability in both cases.P-glycoprotein is associated in many purposes like clearance of xenobiotics compound, transport of small molecules to vital areas, and present in multidrug-resistant malignant cells: its inhibition can be utilized to decrease the multidrug-resistant characteristic. It is also an ABC transporter. On analysis, compounds displayed excellent circumstances in this case. Also, the inhibitory characteristics against P-glycoprotein imply that compound can be applied for the treatment of multidrug-resistant cancer cell lines.

2.7.2 ADMET aqueous solubility

In bioavailability of the drug, the aqueous solubility acts as an essential parameter. At 25° C, it foretells the solubility of the compound in water. Compound holding a PubChem ID: 88265020 confers almost excellent aqueous solubility level by displaying a value of -2.7704 [Table 5]. It indicates that the virtual

screened compound holding a PubChem ID: 88265020 are more polar and more soluble in the aqueous medium correlated with the established compound AEE788 (PubChem ID 10297043).

2.7.3 Compound metabolism

In this section, the expression of the relevant isoforms of cytochrome P450 as a substrate or inhibitor of the virtual screened compound is prognosticated. The compound acts as non-substrate of 2C9, 2D6, and 3A4 isoform of cytochrome P450. In inhibition forecast, it did not expose any inhibitory outcome in 2C9, 2D6, 2C19, and 3A4 isoforms [Table 4] but it displayed in 1A2 isoform of CYP450. Comparison of the score intimates that the virtual screened compound is sufficiently metabolized with respect to cytochrome P450 while comparing with the established compound.

2.7.4 Toxicity prediction

The mutagenicity of a compound is determined by the AMES toxicity test. In the case of the established compound, a negative AMES toxicity test result was designated by the processed ligand compound which indicates that the compound is non-mutagenic. Also, the virtual screened compound is non-carcinogenic and it is showing a lower value contrasted to the established compound. In acute oral toxicity prediction, the virtual screened compound is displaying a slightly higher score compared to the established compound. LD50 dose in the rat model which is the most significant parameter is calculated applying admetSAR. A compound is more lethal when it holds the lower LD50 value compared to a compound having the higher LD50 value. Additionally, it is observed that the virtual screened compound had relatively comparable LD50 value when differentiating with the established compound (2.63 and 2.77 sequentially) [Table 5]. The graphical representation based on parameters HIA, BBB, ADME toxicity, and LD50 is in Fig. 12.

Table 4
Corresponding ADMET profile analysis of the best-established inhibitor (PubChemID:10297043) and best virtual screened compound holding Pub-ChemID 88265020

	Established Compound AEE788 (PubChem ID: 10297043)		Virtual Screened Compound PubChem ID: 88265020	
Model	**Result**	**Probability**	**Result**	**Probability**
Absorption				
Blood-Brain Barrier	BBB+	0.8872	BBB+	0.9262
Human Intestinal Absorption	HIA+	0.9964	HIA+	0.996
Caco-2 Permeability	Caco2-	0.5453	Caco2-	0.638
P-glycoprotein Substrate	Substrate	0.8334	Substrate	0.7012
P-glycoprotein Inhibitor	Inhibitor	0.5299	Non-inhibitor	0.543
	Inhibitor	0.7895	Inhibitor	0.6269
Renal Organic Cation Transporter	Inhibitor	0.6161	Non-inhibitor	0.5375

	Established Compound		Virtual Screened Compound	
Distribution	**Result**	**Probability**	**Result**	**Probability**
Subcellular localization	Nucleus	0.5677	Mitochondria	0.4583
Metabolism				
CYP450 2C9 Substrate	Non-substrate	0.8446	Non-substrate	0.7538
CYP450 2D6 Substrate	Non-substrate	0.696	Non-substrate	0.7285
CYP450 3A4 Substrate	Non-substrate	0.5221	Non-substrate	0.5396
CYP450 1A2 Inhibitor	Non-inhibitor	0.597	Inhibitor	0.6884
CYP450 2C9 Inhibitor	Non-inhibitor	0.7066	Non-inhibitor	0.8274
CYP450 2D6 Inhibitor	Non-inhibitor	0.7209	Non-inhibitor	0.8123
CYP450 2C19 Inhibitor	Non-inhibitor	0.6596	Non-inhibitor	0.8159
CYP450 3A4 Inhibitor	Non-inhibitor	0.8663	Non-inhibitor	0.8503
CYP Inhibitory Promiscuity	High CYP Inhibitory Promiscuity	0.8082	Low CYP Inhibitory Promiscuity	0.5736

	Established Compound		Virtual Screened Compound	
Excretion	**Result**	**Probability**	**Result**	**Probability**
Toxicity				
Human Ether-a-go-go-Related Gene Inhibition	Weak inhibitor	0.6689	Strong inhibitor	0.6529
	Inhibitor	0.8604	Inhibitor	0.75
AMES Toxicity	Non AMES toxic	0.7699	AMES toxic	0.5252
Carcinogens	Non-carcinogens	0.8755	Non-carcinogens	0.7132
Fish Toxicity	High FHMT	0.9324	High FHMT	0.5096
Tetrahymena Pyriformis Toxicity	High TPT	0.9706	High TPT	0.9026
Honey Bee Toxicity	Low HBT	0.8444	Low HBT	0.8037
Biodegradation	Not ready biodegradable	0.9975	Not ready biodegradable	0.9963
Acute Oral Toxicity	III	0.5151	III	0.5992
Carcinogenicity (Three-class)	Non-required	0.6468	Non-required	0.4987

Table 5 ADMET - Regression study

ADMET Predicted Profile — Regression

	Established Compound		Virtual Screened Compound	
Model	Value	Unit	Value	Unit
Absorption				
Aqueous solubility	-3.2214	LogS	-2.7704	LogS
Caco-2 Permeability	0.1928	LogPapp, cm/s	0.2113	LogPapp, cm/s
Distribution				
Metabolism				
Excretion				
Toxicity				
Rat Acute Toxicity	2.778	LD50, mol/kg	2.6319	LD50, mol/kg
Fish Toxicity	1.2483	pLC50, mg/L	1.6451	pLC50, mg/L
Tetrahymena Pyriformis Toxicity	0.6549	pIGC50, ug/L	0.423	pIGC50, ug/L

2.8 Boiled EGG PLOT analysis

Weak bioavailability and pharmacokinetics are result of failures in drug development,apart from ADMET, efficacy, and toxicity. Gastrointestinal consumption and brain access are the foremost two pharmacokinetic exercises central to appraisal at the numerous points of the drug discovery processes. Here, the Brain or IntestinaLEstimateD permeation method (BOILED-Egg) renders a specific forbidding model that estimates the physicochemical properties of small molecules i.e., polarity and lipophilicity [Table 6]. The investigation explicates that the established compound AEE788 (PubChem ID: 10297043) pitching inside the yellow ellipse (i.e. the yolk) exposes the possibility of a high BBB crossing. Whereas, the best Virtual screened compound holding a PubChem ID: 88265020 pitches inside the white ellipse signifying the possibility of huge intestinal absorption [Fig. 13].

Table 6
Best 2 Established Docked compounds and Best 2 Virtual screened compounds used for Boiled Egg plot

Molecule	PubChem ID	MW (g/mol)	TPSA	MLOGP	GI absorption	BBB permeant
AEE-788	10297043	440.58	60.08	3.22	High	Yes
Gefitinib	123631	446.9	68.74	2.82	High	Yes
CID88265020	88265020	569.78	101.13	3.77	High	No
CID71313049	71313049	440.58	60.08	3.22	High	Yes

3. Methodology

3.1 Selection of Inhibitors

The selection of the inhibitors in the prevailing study is a wide search toward discovered inhibitors of VEGF was carried out through various literature studies. Compounds that displayed a capable binding affinity to the protein structure and therefore inhibit its functionality were used for further investigation. 12 established compounds were identified with their unique PubChem ID and their 3D structure available in the database. Table 7 contains the list of all 12 established inhibitors of VEGF with their PubChem ID and other physicochemical properties. The 3D structures of the inhibitors were stored in 3D SDF format.

Table 7
Established VEGF inhibitors with valid 3D structures stored in PubChem

SL. No.	Inhibitors	Pubchem ID	Molecular Weight	H-Bond Donors	H-Bond Acceptors	LogP Value	Ref.
1	Semaxanib	5329098	238.29	2	1	2.5	[9]
2	Vandetanib	3081361	475.362	1	7	4.9	[10]
3	Gefitinib	123631	446.907	1	8	4.1	[11]
4	AEE788	10297043	440.595	2	5	4.6	[12]
5	Parp	16760621	331.8	3	3	-	[13]
6	Pazopanib	10113978	437.522	2	8	3.1	[14]
7	Nintedanib	9809715	539.636	2	7	3.3	[15]
8	Cediranib	9933475	450.514	1	7	4.9	[16]
9	Bevacizumab	24801580	396.153	1	4	-	[17]
10	Sorafenib	216239	464.829	3	7	4.1	[18]
11	Tivozanib	9911830	454.867	2	7	4	[19]
12	Vatalanib	151194	346.818	1	4	4.5	[20]

3.2 Protein and Ligand preparation

Docking studies required a crystal structure of the VEGF protein which was taken from Protein Data Bank (PDB) have a PDB ID: 3V2A [21] and stored for further additional processing to perform the docking process. Additional ligand preparation was introduced along with 3D structures of the established compounds downloaded from the PubChem database was loaded in the LigPrep module of Schrodinger suite, 2013 (Schrodinger. LLC, New York, NY)[22–27]. The process optimization was performed using the OPLS 2005 force field algorithm to get all the compound structures in a single file [28–32]. The obtained file was stored in SDF format and applied for docking studies [33–38].

3.3 Molecular Docking

Molegro Virtual Docker (MVD), the software performs molecular docking and unified high potential Piece-Wise Linear Potential (PLP) and MolDock scoring function [39–44]. The crystal structures of target protein were used for docking and the existing ligand was removed from the protein structure [45–49]. The first cavity was recorded to hold the bound ligand earlier to its elimination and was also observed to have the largest volume and was selected for the further procedure of docking with ligands [50–54]. The single SDF file containing all the 12 ligands created through the LigPrep module was loaded in the docker. Docking procedure parameter was fixed at a maximum iteration of 1500, grid solution 0.2 having a binding affinity and maximum population size 50[55–58]. The protein and ligands were appraised on the subsequent confirmation of the Internal Electrostatic interaction (Internal ES), sp2-sp2 torsions, and internal hydrogen bond interaction. A post dock study included energy minimization and H-bond optimization. Simplex Evolution was fixed at max steps 300 and neighbour distance faster 1.00[59–62]. Nelder Mead Simplex Minimization (using non- grid force field and H-bond directionality) was applied after the docking to minimize the complex energy of ligand-receptor interaction [63–67].

3.4 Virtual screening

Molecular docking produced a re-rank score for every compound which is indicative of the interaction between the compounds with the target protein [22][24]. Compound with a lower re-rank score indicates the effective affinity to the target protein and was confirmed being the best- established compound. A similarity searching of that compound was carried out for determining the best compound having a higher affinity different from any established drugs [68–70]. Therefore, virtual screening was performed against the PubChem database generated by NIH, one of the public chemical repositories which comprise 93 million chemical compounds. The threshold was fixed at > = 95 and filtration property parameter was introduced by the component rule of Lipinski's rule of five. The compound structures were stored in SDF format and were promoted for the molecular docking procedure supported by the same procedure against the crystal structure of the target protein VEGF to recognize the compound possessing exceeded affinity [70–71].

3.5 Molecular Dynamics Simulation

Any molecule in a three-dimensional space has internal motion resulting in conformational change which plays an essential role in their function, this holds true for every biological interaction [72–83]. Hence, molecular dynamic simulation tool is used for scrutinizing details of molecular motion as function of time. The MD-simulation of virtually screened compound and best-established compound provides crucial information on geometrical and thermodynamical aspects of the compound. The simulation was run through 100 ns time step on Schrodinger's Desmond module with OPLS5 force field, which uses an iterative algorithm based on Newtonian dynamic equation. The understanding of structural and functional behaviors of the compound is analyzed through simulation diagram, wherein, RMSD, RMSF, protein-ligand interaction and ligand properties are analyzed[84–96].

3.6 Drug-Drug comparative study

The unnamed complex structures were attain from the docking result of the established compounds and introduced in Molegro Virtual Docker. It was refined by eliminating all the ligands, constraints, and cavities without the protein structure. Subsequent results were recorded to detect the best pose of the best- established compound and then it was imported[97–103]. The structure produced as a consequence was rescued in PDB format. Revaluation of parameters was directed and the data collected was kept in an excel sheet. Similarly, the complex structures were recaptured from the virtual screening result and the same method was iterated. An excel sheet was fixed to investigate all the affinities, hydrogen interaction, steric energy and high re-rank score to recognize the best inhibitor [104–112].

3.7 Pharmacophore studies

Pharmacophore studies comprise different interaction types of ligand and receptor including H-bond interaction, electrostatic interaction, hydrophobic interaction, and aromatic interaction. It is performed by applying Accelrys Discovery Studio 3.5 DS Visualizer. The developed pharmacophore model included the excluded volume spheres, which imitate the inaccessible areas along any potential ligand [113–119].

3.8 Bioactivity and ADMET profiling of compound

Every comparable compound was appraised for their Drug capability by applying Lipinski filter. ADMET represents the pharmacological activity of the compound, which was determined by applying the admetSAR database provides an effective interface to evaluate the biological and chemical profiles. The properties of ADMET profile include adsorption, digestion, metabolism, excretion, and toxicity which perform major roles in the development and discovery of drugs[120–132]. The database comprises of 5 quantitative regression models and 22 qualitative classifications which implement the result with high predictive precision[133–145]. The appraisal of these properties was carried out using admetSAR (http://lmmd.ecust.edu.cn:8000/). The bio-activity properties and toxicity of the two compounds with the highest affinity from the docking and virtual screening studies were predicted using this online admetSAR tool[146–152].

3.9 Boiled-Egg Plot

A Boiled Egg Plot uses the spontaneous and reproducible statistical plot to predict the 2 passive predictions: gastrointestinal (GI) absorption and brain penetration (BBB), which determines its propriety in the development and discovery of drugs. The Cartesian directions of both the ovals were followed to give the dependence data. Also, it contains a few parameters; MW, TPSA, MLOGP, GI, and BBB to restructure the BOILED-Egg plot [76][79]. If in the plot, the compounds of our interest lie on the yellow ellipse, the possibility of the compound penetrating the brain (BBB) is greater indicative of poor compound. Similarly, the compound's Gastrointestinal Absorption (GI) is high if it lies in the white region of the plot indicative of the compound with great absorption capacity [153–162]. Additionally besides these two observations, if the compounds of our interest are placed on the grey area, excluding the yellow ellipse and white areas and are out of range of the plot as well, the compounds are non-absorptive and non-brain penetrative. As per the re-rank affinities, analysis of this plot was performed for the best two inhibitors from the first docking results and the best two compounds obtained from the second docking studies i.e. virtual screening results [163–173]. All these four compounds were considered separately to assess parameters of Gastrointestinal Absorption (GI) and Blood-Brain Barrier (BBB).

Conclusion

Ovarian cancer is the common lethal gynaecologic malignancy and not withstanding many available drugs, this disease is still progressing day by day. Several established compounds which perform as angiogenesis inhibitor are previously identified but the strategy here was to recognize a compound which is more effective than the present drugs. The molecular docking results display the strength of the compound with a PubChem ID: 88265020 to inhibit the VEGF protein. The dynamic simulation compared the conformational changes over a timestep of compound (PubChem ID: 88265020) with the best-established compound. The Electrostatic interaction of the best virtual screened compound and hydrophobic forces enclosing it with a large number of hydrogen bonding interactions with the amino acid debris promotes productive pharmacophoric interplays. The boiled egg-plot investigation stipulates that the best virtual screened compound is located in the white area of the plot symbolizing peculiar intestinal absorption. The foregoing qualities decide that the best virtual screened drug is actively bioavailable. Therefore, the information suggests that the best virtual screened compound have an essential inhibitory effect against the target protein VEGF. Additionally, the aforementioned investigation presents a field for the examination of the compound with PubChem ID: 88265020 to be investigated for the prevention of ovarian cancer. It indicates a compound with a PubChem ID: 88265020 inhibit VEGF more strongly than the established drug AEE788. Moreover, *In vitro* study might acknowledge the aforementioned drug as a hopeful chapter in ovarian carcinoma.

Declarations

Funding/Acknowledgment

1. This work was supported by the Taif University Researchers Supporting Program (Project number: TURSP-2020/151), Taif University, Saudi Arabia.
2. The authors are grateful to the Deanship of Scientific Research, King Saud University for funding through Vice Deanship of Scientific Research Chairs.
3. SKS thank Alagappa University, Department of Biotechnology (DBT), New Delhi (No. BT/PR8138/BID/7/458/2013, dated 23rd May, 2013), DST-PURSE 2nd Phase Programme Order No. SR/PURSE Phase 2/38 (G dated 21.02.2017 and FIST (SR/FST/LSI - 667/2016), MHRD RUSA 1.0 and RUSA 2.0 for providing the financial assistance. UP gratefully acknowledge Indian Council of Medical Research (ISRM/11/(19)/2017, dated: 09.08.2018).
4. SKS thankfully acknowledges the Tamil Nadu State Council for Higher Education (TANSCHE) for the research grant (Au/S.o. (P&D): TANSCHE Projects: 117/2021).

AUTHOR CONTRIBUTIONS

SM contributed equally to this work with MA.SM and MA was involved in Molecular docking, Molecular Dynamics Simulation, Writing – review & editing. LP, AP, AC and MM were contributed towards Inhibitors collection, Datacuration, Formal analysis, Validation, Visualization. MY, RK, AAB and TH were involved in Molecular Docking, ADMET analysis, R Programming analysis, Writing – review & editing. AN, AAB, TH and SKS were contributed in investigation, supervision, writing – review & editing

Conflicts of interest/Competing interests:

The authors declare that they have no conflict ofinterest.

AVAILABILITY OF DATA AND MATERIALS:

Not applicable.

Code Availability:

Code will be provided as per the request

ETHICS APPROVAL AND CONSENT TO PARTICIPATE:

Not applicable.

HUMAN AND ANIMAL RIGHTS:

No animals/humans were used in the studies that are the basis of this research.

References

1. Tew, W. P. (2016). "Ovarian cancer in the older woman."JGeriatr Oncol7(5): 354-361.

2. Tiper, I. V., et al. (2016). "VEGF potentiates GD3-mediated immune suppression by human ovarian cancer cells."Clinical Cancer Research: clincanres. 2518.2015.
3. Weiderpass, E. and J. E. Tyczynski (2015). "Epidemiology of patients with ovarian cancer with and without a BRCA1/2 Mutation."Molecular diagnosis & therapy19(6): 351-364.
4. Premalata, C., et al. (2016). "Expression of VEGF-A in Epithelial Ovarian Cancer: Correlation with Morphologic Types, Grade and Clinical Stage."The Gulf journal of oncology1(21): 49-54.
5. Horikawa, N., et al. (2017). "Expression of vascular endothelial growth factor in ovarian cancer inhibits tumor immunity through the accumulation of myeloid-derived suppressor cells."Clinical Cancer Research23(2): 587-599.
6. Tino, A. B., et al. (2016). "Resveratrol and acetyl-resveratrol modulate activity of VEGF and IL-8 in ovarian cancer cell aggregates via attenuation of the NF-κBprotein."Journal of ovarian research9(1): 84.
7. Grunewald, T. and J. A. Ledermann (2017). "Targeted therapies for ovarian cancer."Best Practice & Research Clinical Obstetrics & Gynaecology41: 139-152.
8. Choi, H.-J., et al. (2015). "Anti-vascular therapies in ovarian cancer: moving beyond anti-VEGF approaches."Cancer and Metastasis Reviews34(1): 19-40.
9. Belotti, D., et al. (2003). "Matrix metalloproteinases (MMP9 and MMP2) induce the release of vascular endothelial growth factor (VEGF) by ovarian carcinoma cells: implications for ascites formation."Cancer Res63(17): 5224-5229.
10. Wedge, S. R., et al. (2002). "ZD6474 inhibits vascular endothelial growth factor signaling, angiogenesis, and tumor growth following oral administration."Cancer Res62(16): 4645-4655.
11. Ciardiello, F., et al. (2001). "Inhibition of growth factor production and angiogenesis in human cancer cells by ZD1839 (Iressa), a selective epidermal growth factor receptor tyrosine kinase inhibitor."Clinical Cancer Research7(5): 1459-1465.
12. Traxler, P., et al. (2004). "AEE788: a dual family epidermal growth factor receptor/ErbB2 and vascular endothelial growth factor receptor tyrosine kinase inhibitor with antitumor and antiangiogenic activity."Cancer Res64(14): 4931-4941.
13. Liu, J., et al. (2018). "Assessment and management of diarrhea following VEGF receptor TKI treatment in patients with ovarian cancer."Gynecologic oncology.
14. Richardson, D. L., et al. (2018). "Paclitaxel with and without pazopanib for persistent or recurrent ovarian cancer: a randomized clinical trial."JAMA oncology4(2): 196-202.
15. Khalique, S. and S. Banerjee (2017). "Nintedanib in ovarian cancer."Expert opinion on investigational drugs26(9): 1073-1081.
16. Orbegoso, C., et al. (2017). "The role of Cediranib in ovarian cancer."Expert opinion on pharmacotherapy18(15): 1637-1648.
17. Zhang, W., et al. (2017). "The benefits and side effects of bevacizumab for the treatment of recurrent ovarian cancer."Current drug targets18(10): 1125-1131.

18. Azad, N. S., et al. (2008). "Combination targeted therapy with sorafenib and bevacizumab results in enhanced toxicity and antitumor activity."Journal of Clinical Oncology26 (22): 3709-3714.
19. Nakamura, K., et al. (2006). "KRN951, a highly potent inhibitor of vascular endothelial growth factor receptor tyrosine kinases, has antitumor activities and affects functional vascular properties."Cancer Res66(18): 9134-9142.
20. Xu, L., et al. (2000). "Inhibition of malignant ascites and growth of human ovarian carcinoma by oral administration of a potent inhibitor of the vascular endothelial growth factor receptor tyrosine kinases."International journal of oncology16(3): 445-499.
21. Brozzo, M. S., et al. (2012). "Thermodynamic and structural description of allosterically regulated VEGFR-2 dimerization."Blood119(7): 1781-1788.
22. Sharma, K., Patidar, K., Ali, M.A., Patil, P., Goud, H., Hussain, T., Nayarisseri, A. and Singh, S.K. (2018). Structure-based virtual screening for the identification of high affinity compounds as potent VEGFR2 inhibitors for the treatment of renal cell carcinoma. Current topics in medicinal chemistry, 18(25), 2174-2185.
23. Sahila, M. M., Babitha, P. P., Bandaru, S., Nayarisseri, A., & Doss, V. A. (2015). Molecular docking based screening of GABA (A) receptor inhibitors from plant derivatives. Bioinformation, 11(6), 280.
24. Vuree, S., Dunna, N.R., Khan, I.A., Alharbi, K.K., Vishnupriya, S., Soni, D., Shah, P., Chandok, H., Yadav, M. and Nayarisseri, A. (2013). Pharmacogenomics of drug resistance in Breast Cancer Resistance Protein (BCRP) and its mutated variants. journal of pharmacy research, 6(7), 791-798.
25. Monteiro, A. F. M., Viana, J. D. O., Nayarisseri, A., Zondegoumba, E. N., Mendonça Junior, F. J. B., Scotti, M. T., & Scotti, L. (2018). Computational studies applied to flavonoids against alzheimer's and parkinson's diseases. Oxidative medicine and cellular longevity, 2018.
26. Bandaru, S., GangadharanSumithnath, T., Sharda, S., Lakhotia, S., Sharma, A., Jain, A., Hussain, T., Nayarisseri, A. and Kumar Singh, S. (2017). Helix-Coil transition signatures B-Raf V600E mutation and virtual screening for inhibitors directed against mutant B-Raf. Current drug metabolism, 18(6), 527-534.
27. Kelotra, A., Gokhale, S.M., Kelotra, S., Mukadam, V., Nagwanshi, K., Bandaru, S., Nayarisseri, A. and Bidwai, A. (2014). Alkyloxy carbonyl modified hexapeptides as a high affinity compounds for Wnt5A protein in the treatment of psoriasis. Bioinformation, 10(12), 743.
28. Basak, S. C., Nayarisseri, A., González-Díaz, H., &Bonchev, D. (2016). Editorial (Thematic Issue: chemoinformatics models for pharmaceutical design, part 1). 22(33):5041-5042.
29. Basak, S. C., Nayarisseri, A., González-Díaz, H., &Bonchev, D. (2016). Editorial (Thematic Issue: Chemoinformatics models for pharmaceutical design, part 2). 22(34):5177-5178.
30. Prajapati, L., Khandelwal, R., Yogalakshmi, K. N., Munshi, A., &Nayarisseri, A. (2020). Computer-aided Structure prediction of Bluetongue Virus coat protein VP2 assisted by Optimized Potential for Liquid Simulations (OPLS). Current topics in medicinal chemistry, 20(19), 1720-1732.
31. Nayarisseri, A., Khandelwal, R., Madhavi, M., Selvaraj, C., Panwar, U., Sharma, K., Hussain, T. and Singh, S.K. (2020). Shape-based machine learning models for the potential novel COVID-19 protease

inhibitors assisted by molecular dynamics simulation. Current topics in medicinal chemistry, 20(24), 2146-2167.

32. Nayarisseri, A. (2020). Most Promising Compounds for Treating COVID-19 and Recent Trends in Antimicrobial & Antifungal Agents. Current topics in medicinal chemistry, 20(24), 2119-2125.
33. Pochetti, G., Mitro, N., Lavecchia, A., Gilardi, F., Besker, N., Scotti, E., Aschi, M., Re, N., Fracchiolla, G., Laghezza, A. and Tortorella, P. (2010). Structural insight into peroxisome proliferator-activated receptor γ binding of two ureidofibrate-like enantiomers by molecular dynamics, cofactor interaction analysis, and site-directed mutagenesis. Journal of medicinal chemistry, 53(11), 4354-4366.
34. Soares Rodrigues, G. C., dos Santos Maia, M., Muratov, E. N., Scotti, L., & Scotti, M. T. (2020). Quantitative Structure–Activity Relationship Modeling and Docking of Monoterpenes with Insecticidal Activity Against Reticulitermes chinensis Snyder and Drosophila melanogaster. Journal of agricultural and food chemistry, 68(16), 4687-4698.
35. Wang, Y., Wang, L. F., Zhang, L. L., Sun, H. B., & Zhao, J. (2020). Molecular mechanism of inhibitor bindings to bromodomain-containing protein 9 explored based on molecular dynamics simulations and calculations of binding free energies. SAR and QSAR in Environmental Research, 31(2), 149-170.
36. Wang, L. F., Wang, Y., Yang, Z. Y., Zhao, J., Sun, H. B., & Wu, S. L. (2020). Revealing binding selectivity of inhibitors toward bromodomain-containing proteins 2 and 4 using multiple short molecular dynamics simulations and free energy analyses. SAR and QSAR in Environmental Research, 31(5), 373-398.
37. Brugnoni, M., Scotti, A., Rudov, A.A., Gelissen, A.P., Caumanns, T., Radulescu, A., Eckert, T., Pich, A., Potemkin, I.I. and Richtering, W. (2018). Swelling of a responsive network within different constraints in multi-thermosensitive microgels. Macromolecules, 51(7), 2662-2671.
38. Montanari, R., Saccoccia, F., Scotti, E., Crestani, M., Godio, C., Gilardi, F., Loiodice, F., Fracchiolla, G., Laghezza, A., Tortorella, P. and Lavecchia, A. (2008). Crystal structure of the peroxisome proliferator-activated receptor γ (PPARγ) ligand binding domain complexed with a novel partial agonist: a new region of the hydrophobic pocket could be exploited for drug design. Journal of medicinal chemistry, 51(24), 7768-7776.
39. Wang, J., Qian, Y., Li, L., &Qiu, X. (2020). Atomic Force Microscopy and Molecular Dynamics Simulations for Study of Lignin Solution Self-Assembly Mechanisms in Organic–Aqueous Solvent Mixtures. ChemSusChem, 13(17), 4420-4427.
40. Liguori, N., Croce, R., Marrink, S. J., &Thallmair, S. (2020). Molecular dynamics simulations in photosynthesis. Photosynthesis research, 144(2), 273-295.
41. Kuzmanic, A., Bowman, G. R., Juarez-Jimenez, J., Michel, J., &Gervasio, F. L. (2020). Investigating cryptic binding sites by molecular dynamics simulations. Accounts of chemical research, 53(3), 654-661.
42. Klesse, G., Rao, S., Tucker, S. J., & Sansom, M. S. (2020). Induced polarization in molecular dynamics simulations of the 5-HT3 receptor channel. Journal of the American Chemical Society, 142(20), 9415-9427.

43. Shiau, A. K., Barstad, D., Loria, P. M., Cheng, L., Kushner, P. J., Agard, D. A., & Greene, G. L. (1998). The structural basis of estrogen receptor/coactivator recognition and the antagonism of this interaction by tamoxifen. Cell, 95(7), 927-937.
44. Berman, H., Henrick, K., Nakamura, H., & Markley, J. L. (2007). The worldwide Protein Data Bank (wwPDB): ensuring a single, uniform archive of PDB data. Nucleic acids research, 35(suppl_1), D301-D303.
45. Natchimuthu, V., Bandaru, S., Nayarisseri, A., & Ravi, S. (2016). Design, synthesis and computational evaluation of a novel intermediate salt of N-cyclohexyl-N-(cyclohexylcarbamoyl)-4-(trifluoromethyl) benzamide as potential potassium channel blocker in epileptic paroxysmal seizures. Computational biology and chemistry, 64, 64-73.
46. Bandaru, S., Alvala, M., Akka, J., Sagurthi, S. R., Nayarisseri, A., Kumar Singh, S., & Prasad Mundluru, H. (2016). Identification of small molecule as a high affinity β2 agonist promiscuously targeting wild and mutated (Thr164Ile) β 2 adrenergic receptor in the treatment of bronchial asthma. Current pharmaceutical design, 22(34), 5221-5233.
47. Majhi, M., Ali, M.A., Limaye, A., Sinha, K., Bairagi, P., Chouksey, M., Shukla, R., Kanwar, N., Hussain, T., Nayarisseri, A. and Singh, S.K (2018). An in silico investigation of potential EGFR inhibitors for the clinical treatment of colorectal cancer. Current topics in medicinal chemistry, 18(27), 2355-2366.
48. Khandelwal, R., Chauhan, A.P., Bilawat, S., Gandhe, A., Hussain, T., Hood, E.A., Nayarisseri, A. and Singh, S.K. (2018). Structure-based virtual screening for the identification of high-affinity small molecule towards STAT3 for the clinical treatment of osteosarcoma. Current topics in medicinal chemistry, 18(29), 2511-2526.
49. Sinha, K., Majhi, M., Thakur, G., Patidar, K., Sweta, J., Hussain, T., Nayarisseri, A. and Singh, S.K. (2018). Computer-aided drug designing for the identification of high-affinity small molecule targeting cd20 for the clinical treatment of chronic lymphocytic leukemia (CLL). Current topics in medicinal chemistry, 18(29), 2527-2542.
50. Chandrakar, B., Jain, A., Roy, S., Gutlapalli, V.R., Saraf, S., Suppahia, A., Verma, A., Tiwari, A., Yadav, M. and Nayarisseri, A. (2013). Molecular modeling of Acetyl-CoA carboxylase (ACC) from Jatropha curcas and virtual screening for identification of inhibitors. journal of pharmacy research, 6(9), 913-918.
51. Nayarisseri, A., Moghni, S. M., Yadav, M., Kharate, J., Sharma, P., Chandok, K. H., & Shah, K. P. (2013). In silico investigations on HSP90 and its inhibition for the therapeutic prevention of breast cancer. journal of pharmacy research, 7(2), 150-156.
52. Udhwani, T., Mukherjee, S., Sharma, K., Sweta, J., Khandekar, N., Nayarisseri, A., & Singh, S. K. (2019). Design of PD-L1 inhibitors for lung cancer. Bioinformation, 15(2), 139.
53. Shukla, P., Khandelwal, R., Sharma, D., Dhar, A., Nayarisseri, A., & Singh, S. K. (2019). Virtual screening of IL-6 inhibitors for idiopathic arthritis. Bioinformation, 15(2), 121.
54. Nayarisseri, A., & Hood, E. A. (2018). Advancement in microbial cheminformatics. Current topics in medicinal chemistry, 18(29), 2459-2461.

55. Jain, D., Udhwani, T., Sharma, S., Gandhe, A., Reddy, P. B., Nayarisseri, A., & Singh, S. K. (2019). Design of novel JAK3 Inhibitors towards Rheumatoid Arthritis using molecular docking analysis. Bioinformation, 15(2), 68.
56. Nayarisseri, A., & Singh, S. K. (2019). Functional inhibition of VEGF and EGFR suppressors in cancer treatment. Current topics in medicinal chemistry, 19(3), 178-179.
57. Gokhale, P., Chauhan, A. P. S., Arora, A., Khandekar, N., Nayarisseri, A., & Singh, S. K. (2019). FLT3 inhibitor design using molecular docking based virtual screening for acute myeloid leukemia. Bioinformation, 15(2), 104.
58. Ali, M. A., Vuree, S., Goud, H., Hussain, T., Nayarisseri, A., & Singh, S. K. (2019). Identification of high-affinity small molecules targeting gamma secretase for the treatment of Alzheimer's disease. Current topics in medicinal chemistry, 19(13), 1173-1187.
59. Patidar, K., Panwar, U., Vuree, S., Sweta, J., Sandhu, M. K., Nayarisseri, A., & Singh, S. K. (2019). An in silico approach to identify high affinity small molecule targeting m-TOR inhibitors for the clinical treatment of breast cancer. Asian Pacific journal of cancer prevention: APJCP, 20(4), 1229.
60. Pandey, N., Yadav, M., Nayarisseri, A., Ojha, M., Prajapati, J., & Gupta, S. (2013). Cross evaluation of different classes of alpha-adrenergic receptor antagonists to identify overlapping pharmacophoric requirements. journal of pharmacy research, 6(1), 173-178.
61. Marunnan, S. M., Pulikkal, B. P., Jabamalairaj, A., Bandaru, S., Yadav, M., Nayarisseri, A., & Doss, V. A. (2017). Development of MLR and SVM aided QSAR models to identify common SAR of GABA uptake herbal inhibitors used in the treatment of Schizophrenia. Current neuropharmacology, 15(8), 1085-1092.
62. Sweta, J., Khandelwal, R., Srinitha, S., Pancholi, R., Adhikary, R., Ali, M. A., ... & Singh, S. K. (2019). Identification of high-affinity small molecule targeting IDH2 for the clinical treatment of acute myeloid leukemia. Asian Pacific journal of cancer prevention: APJCP, 20(8), 2287.
63. Nayarisseri, A. (2019). Prospects of utilizing computational techniques for the treatment of human diseases. Current topics in medicinal chemistry, 19(13), 1071-1074.
64. Schrodinger, LLC, NY, USA, 2009
65. LigPrep, Schrodinger LLC, Ney York, NY.
66. Prime, Schrodinger, LLC, Ney York, NY.
67. Protein Preparation Wizard, Schrodinger, LLC, Ney York, NY.
68. Qikprop, Schrodinger, LLC, Ney York, NY.
69. Shelley, J. C., Cholleti, A., Frye, L. L., Greenwood, J. R., Timlin, M. R., &Uchimaya, M. (2007). Epik: a software program for pK a prediction and protonation state generation for drug-like molecules. Journal of computer-aided molecular design, 21(12), 681-691.
70. Baby, K., Maity, S., Mehta, C. H., Suresh, A., Nayak, U. Y., & Nayak, Y. (2020). Targeting SARS-CoV-2 main protease: A computational drug repurposing study. Archives of medical research.

71. Gahlawat, A., Kumar, N., Kumar, R., Sandhu, H., Singh, I. P., Singh, S., ... & Garg, P. (2020). Structure-based virtual screening to discover potential lead molecules for the SARS-CoV-2 main protease. Journal of chemical information and modeling.
72. ShivanikaC , Deepak Kumar S. , VenkataraghavanRagunathan , Pawan Tiwari , Sumitha A. &Brindha Devi P (2020): Molecular docking, validation, dynamics simulations, and pharmacokinetic prediction of natural compounds against the SARS-CoV-2 main-protease, Journal of Biomolecular Structure and Dynamics, DOI: 10.1080/07391102.2020.1815584]
73. Karplus, M., & McCammon, J. A. (2002). Molecular dynamics simulations of biomolecules. Nature structural biology, 9(9), 646-652.
74. Satyajit Beura&Chetti Prabhakar (2020): In-silico strategies for probing chloroquine based inhibitors against SARS-CoV-2, Journal of Biomolecular Structure and Dynamics, DOI: 10.1080/07391102.2020.1772111Xu, X., Mao, L., Xu, W., Tang, W., Zhang, X., Xi, B., ... & Zhang, L. (2016). AC0010, an irreversible EGFR inhibitor selectively targeting mutated EGFR and overcoming T790M-induced resistance in animal models and lung cancer patients. Molecular cancer therapeutics, 15(11), 2586-2597.
75. Sharda, S., Khandelwal, R., Adhikary, R., Sharma, D., Majhi, M., Hussain, T., ... & Singh, S. K. (2019). A Computer-Aided Drug Designing for Pharmacological Inhibition of Mutant ALK for the Treatment of Non-small Cell Lung Cancer. Current topics in medicinal chemistry, 19(13), 1129-1144.
76. Limaye, A., Sweta, J., Madhavi, M., Mudgal, U., Mukherjee, S., Sharma, S., Hussain, T., Nayarisseri, A. and Singh, S.K. (2019). In silico insights on gd2: a potential target for pediatric neuroblastoma. Current topics in medicinal chemistry, 19(30), 2766-2781.
77. Nayarisseri, A., & Yadav, M. (2015). Editorial (Thematic Issue: Mechanistics in drug design-experimental molecular biology vs. molecular modeling). Current topics in medicinal chemistry, 15(1), 3-4.
78. Kleandrova, V. V., Scotti, M. T., Scotti, L., Nayarisseri, A., & Speck-Planche, A. (2020). Cell-based multi-target QSAR model for design of virtual versatile inhibitors of liver cancer cell lines. SAR and QSAR in Environmental Research, 31(11), 815-836.
79. Nayarisseri, A. (2020). Experimental and computational approaches to improve binding affinity in chemical biology and drug discovery. Current Topics in Medicinal Chemistry, 20(19), 1651-1660.
80. Kaushik, A. C., Kumar, S., Wei, D. Q., &Sahi, S. (2018). Structure based virtual screening studies to identify novel potential compounds for GPR142 and their relative dynamic analysis for study of type 2 diabetes. Frontiers in chemistry, 6, 23.
81. Toledo Warshaviak, D., Golan, G., Borrelli, K. W., Zhu, K., &Kalid, O. (2014). Structure-based virtual screening approach for discovery of covalently bound ligands. Journal of chemical information and modeling, 54(7), 1941-1950.
82. Lyne, P. D. (2002). Structure-based virtual screening: an overview. Drug discovery today, 7(20), 1047-1055.

83. Dighe, S.N., Deora, G.S., De la Mora, E., Nachon, F., Chan, S., Parat, M.O., Brazzolotto, X. and Ross, B.P. (2016). Discovery and structure–activity relationships of a highly selective butyrylcholinesterase inhibitor by structure-based virtual screening. Journal of medicinal chemistry, 59(16), 7683-7689.
84. Schrödinger, L. (2011). QikProp: Rapid ADME predictions of drug candidates.
85. Lionta, E., Spyrou, G., K Vassilatis, D., &Cournia, Z. (2014). Structure-based virtual screening for drug discovery: principles, applications and recent advances. Current topics in medicinal chemistry, 14(16), 1923-1938.
86. Vidler, L.R., Filippakopoulos, P., Fedorov, O., Picaud, S., Martin, S., Tomsett, M., Woodward, H., Brown, N., Knapp, S. and Hoelder, S. (2013). Discovery of novel small-molecule inhibitors of BRD4 using structure-based virtual screening. Journal of medicinal chemistry, 56(20), 8073-8088.
87. Pitt, W. R., Calmiano, M. D., Kroeplien, B., Taylor, R. D., Turner, J. P., & King, M. A. (2013). Structure-based virtual screening for novel ligands. In Protein-Ligand Interactions (pp. 501-519). Humana Press, Totowa, NJ.
88. Choudhary, S., Malik, Y. S., &Tomar, S. (2020). Identification of SARS-CoV-2 cell entry inhibitors by drug repurposing using in silico structure-based virtual screening approach. Frontiers in immunology, 11, 1664.
89. Adhikary R, Khandelwal R, Hussain T, Nayarisseri A, Singh SK. Structural Insights into the Molecular Design of ROS1 Inhibitor for the Treatment of Non-Small Cell Lung Cancer (NSCLC). Current Computer-aided Drug Design. 2020 May. DOI: 10.2174/1573409916666200504105249.
90. Aher, A., Udhwani, T., Khandelwal, R., Limaye, A., Hussain, T., Nayarisseri, A., & Singh, S. K. (2020). In silico insights on IL-6: A potential target for multicentric castleman disease. Current computer-aided drug design, 16(5), 641-653.
91. Qureshi S, Khandelwal R, Madhavi M, et al. A Multi-Target Drug Designing for BTK, MMP9, Proteasome And TAK1 for the clinical treatment of Mantle Cell Lymphoma. Current Topics in Medicinal Chemistry. 2021 Jan. DOI: 10.2174/1568026621666210119112336.
92. Yadav, M., Khandelwal, R., Mudgal, U., Srinitha, S., Khandekar, N., Nayarisseri, A., ... & Singh, S. K. (2019). Identification of Potent VEGF Inhibitors for the Clinical Treatment of Glioblastoma, A Virtual Screening Approach. Asian Pacific journal of cancer prevention: APJCP, 20(9), 2681.
93. Nayarisseri A, Khandelwal R, Tanwar P, Madhavi M, Sharma D, Thakur G, Speck-Planche A, Singh SK. Artificial Intelligence, Big data and Machine Learning approaches in Precision Medicine & Drug Discovery. Curr Drug Targets. 2021 Jan 4. doi: 10.2174/1389450122999210104205732. Epub ahead of print. PMID: 33397265.
94. Francisco J. B. Mendonça-Junior, Marcus T. Scotti, AnurajNayarisseri, Ernestine N. T. Zondegoumba, Luciana Scotti, "Natural Bioactive Products with Antioxidant Properties Useful in Neurodegenerative Diseases", Oxidative Medicine and Cellular Longevity, vol. 2019, Article ID 7151780, 2 pages, 2019. https://doi.org/10.1155/2019/7151780
95. Celik, I., Erol, M., TemizArpaci, O., SezerSenol, F., & Erdogan Orhan, I. (2020). Evaluation of activity of some 2, 5-disubstituted benzoxazole derivatives against acetylcholinesterase, butyrylcholinesterase

and tyrosinase: ADME prediction, DFT and comparative molecular docking studies. Polycyclic Aromatic Compounds, 1-12.

96. Pawar, V.S., Lokwani, D.K., Bhandari, S.V., Bothara, K.G., Chitre, T.S., Devale, T.L., Modhave, N.S. and Parikh, J.K., 2011. (2011). Design, docking study and ADME prediction of Isatin derivatives as anti-HIV agents. Medicinal chemistry research, 20(3), 370-380.
97. Dincel, E. D., Gürsoy, E., Yilmaz-Ozden, T., &Ulusoy-Güzeldemirci, N. (2020). Antioxidant activity of novel imidazo [2, 1-b] thiazole derivatives: Design, synthesis, biological evaluation, molecular docking study and in silico ADME prediction. Bioorganic Chemistry, 103, 104220.
98. Kumar, S., Saini, V., Maurya, I. K., Sindhu, J., Kumari, M., Kataria, R., & Kumar, V. (2018). Design, synthesis, DFT, docking studies and ADME prediction of some new coumarinyl linked pyrazolylthiazoles: Potential standalone or adjuvant antimicrobial agents. PloS one, 13(4), e0196016.
99. Erol, M., Celik, I., Temiz-Arpaci, O., Goker, H., Kaynak-Onurdag, F., &Okten, S. (2020). Synthesis, molecular docking and ADME prediction of some new benzimidazole carboxamidines derivatives as antimicrobial agents. Medicinal Chemistry Research, 29(11), 2028-2038.
100. Kashid, A. M., Dube, P. N., Alkutkar, P. G., Bothara, K. G., Mokale, S. N., & Dhawale, S. C. (2013). Synthesis, biological screening and ADME prediction of benzylindole derivatives as novel anti-HIV-1, anti-fungal and anti-bacterial agents. Medicinal Chemistry Research, 22(10), 4633-4640.
101. Kalin, T. N., Kilic, D., Arslan, F., Colak, O., &Altundas, A. (2020). Synthesis, molecular modeling studies, ADME prediction of arachidonic acid carbamate derivatives, and evaluation of their acetylcholinesterase activity. Drug development research, 81(2), 232-241.
102. Kumar, A., Rathi, E., &Kini, S. G. (2019). E-pharmacophore modelling, virtual screening, molecular dynamics simulations and in-silico ADME analysis for identification of potential E6 inhibitors against cervical cancer. Journal of Molecular Structure, 1189, 299-306.
103. Bhatt, J. D., Chudasama, C. J., & Patel, K. D. (2015). Pyrazole clubbed triazolo [1, 5-a] pyrimidine hybrids as an anti-tubercular agents: Synthesis, in vitro screening and molecular docking study. Bioorganic & medicinal chemistry, 23(24), 7711-7716.
104. Dofe, V. S., Sarkate, A. P., Lokwani, D. K., Shinde, D. B., Kathwate, S. H., & Gill, C. H. (2017). Novel O-Alkylated Chromones as Antimicrobial Agents: Ultrasound Mediated Synthesis, Molecular Docking and ADME Prediction. Journal of Heterocyclic Chemistry, 54(5), 2678-2685.
105. Malik, R., Mehta, P., Srivastava, S., Choudhary, B. S., & Sharma, M. (2017). Pharmacophore modeling, 3D-QSAR, and in silico ADME prediction of N-pyridyl and pyrimidine benzamides as potent antiepileptic agents. Journal of Receptors and Signal Transduction, 37(3), 259-266.
106. da Silva Hage-Melim, L. I., Federico, L. B., de Oliveira, N. K. S., Francisco, V. C. C., Correia, L. C., de Lima, H. B., ... &Francischini, I. A. G. (2020). Virtual screening, ADME/Tox predictions and the drug repurposing concept for future use of old drugs against the COVID-19. Life Sciences, 256, 117963.
107. Upadhyay, S., Tripathi, A. C., Paliwal, S., & Saraf, S. K. (2017). 2-pyrazoline derivatives in neuropharmacology: Synthesis, ADME prediction, molecular docking and in vivo biological

evaluation. EXCLI journal, 16, 628.

108. Pandey, R.K., Narula, A., Naskar, M., Srivastava, S., Verma, P., Malik, R., Shah, P. and Prajapati, V.K., (2017). Exploring dual inhibitory role of febrifugine analogues against Plasmodium utilizing structure-based virtual screening and molecular dynamic simulation. Journal of Biomolecular Structure and Dynamics, 35(4), 791-804.
109. Sadhasivam, A., & Vetrivel, U. (2019). Identification of potential drugs targeting L, L-diaminopimelate aminotransferase of Chlamydia trachomatis: An integrative pharmacoinformatics approach. Journal of cellular biochemistry, 120(2), 2271-2288.
110. Zakerali, T., &Shahbazi, S. (2018). Rational druggability investigation toward selection of lead molecules: impact of the commonly used spices on inflammatory diseases. Assay and drug development technologies, 16(7), 397-407.
111. Suma, K. B., Kumari, A., Shetty, D., Fernandes, E., Chethan, D. V., Jays, J., &Murahari, M. (2020). Structure based pharmacophore modelling approach for the design of azaindole derivatives as DprE1 inhibitors for tuberculosis. Journal of Molecular Graphics and Modelling, 101, 107718.
112. Sukumar, N., &Pask, J. E. (2009). Classical and enriched finite element formulations for Bloch-periodic boundary conditions. International Journal for Numerical Methods in Engineering, 77(8), 1121-1138.
113. Rohini, K., Ramanathan, K., & Shanthi, V. (2019). Multi-dimensional screening strategy for drug repurposing with statistical framework—a new road to influenza drug discovery. Cell biochemistry and biophysics, 77(4), 319-333.
114. Halgren, T. A., Murphy, R. B., Friesner, R. A., Beard, H. S., Frye, L. L., Pollard, W. T., & Banks, J. L. (2004). Glide: a new approach for rapid, accurate docking and scoring. 2. Enrichment factors in database screening. Journal of medicinal chemistry, 47(7), 1750-1759.
115. Sastry, G. M., Adzhigirey, M., Day, T., Annabhimoju, R., & Sherman, W. (2013). Protein and ligand preparation: parameters, protocols, and influence on virtual screening enrichments. Journal of computer-aided molecular design, 27(3), 221-234.
116. Lenselink, E. B., Beuming, T., Sherman, W., van Vlijmen, H. W., &IJzerman, A. P. (2014). Selecting an optimal number of binding site waters to improve virtual screening enrichments against the adenosine A2A receptor. Journal of chemical information and modeling, 54(6), 1737-1746.
117. Verma, P., Tiwari, M., & Tiwari, V. (2018). In silico high-throughput virtual screening and molecular dynamics simulation study to identify inhibitor for AdeABC efflux pump of Acinetobacter baumannii. Journal of Biomolecular Structure and Dynamics, 36(5), 1182-1194.
118. Sherman, W., Beard, H. S., & Farid, R. (2006). Use of an induced fit receptor structure in virtual screening. Chemical biology & drug design, 67(1), 83-84.
119. Bhachoo, J., &Beuming, T. (2017). Investigating protein–peptide interactions using the Schrödinger computational suite. Modeling peptide-protein interactions, 235-254.
120. Deb, P. K., Chandrasekaran, B., Mailavaram, R., Tekade, R. K., & Jaber, A. M. Y. (2019). Molecular modeling approaches for the discovery of adenosine A2B receptor antagonists: current status and

future perspectives. Drug discovery today, 24(9), 1854-1864.

121. Vanajothi, R., Hemamalini, V., Jeyakanthan, J., &Premkumar, K. (2020). Ligand-based pharmacophore mapping and virtual screening for identification of potential discoidin domain receptor 1 inhibitors. Journal of Biomolecular Structure and Dynamics, 38(9), 2800-2808.
122. Politi, A., Durdagi, S., Moutevelis-Minakakis, P., Kokotos, G., &Mavromoustakos, T. (2010). Development of accurate binding affinity predictions of novel renin inhibitors through molecular docking studies. Journal of Molecular Graphics and Modelling, 29(3), 425-435.
123. Liu, K., &Kokubo, H. (2017). Exploring the stability of ligand binding modes to proteins by molecular dynamics simulations: a cross-docking study. Journal of chemical information and modeling, 57(10), 2514-2522.
124. Munnaluri, R., Sivan, S. K., & Manga, V. (2015). Molecular docking and MM/GBSA integrated protocol for designing small molecule inhibitors against HIV-1 gp41. Medicinal Chemistry Research, 24(2), 829-841.
125. Lyne, P. D., Lamb, M. L., &Saeh, J. C. (2006). Accurate prediction of the relative potencies of members of a series of kinase inhibitors using molecular docking and MM-GBSA scoring. Journal of medicinal chemistry, 49(16), 4805-4808.
126. Peddi, S. R., Sivan, S. K., & Manga, V. (2018). Molecular dynamics and MM/GBSA-integrated protocol probing the correlation between biological activities and binding free energies of HIV-1 TAR RNA inhibitors. Journal of Biomolecular Structure and Dynamics, 36(2), 486-503.
127. Feixiong Cheng, Weihua Li, Yadi Zhou, Jie Shen, Zengrui Wu, Guixia Liu, Philip W. Lee, Yun Tang. admetSAR: a comprehensive source and free tool for evaluating chemical ADMET properties. J. Chem. Inf. Model., 2012, 52(11): 3099-3105.
128. Shen, M., Zhou, S., Li, Y., Pan, P., Zhang, L., & Hou, T. (2013). Discovery and optimization of triazine derivatives as ROCK1 inhibitors: molecular docking, molecular dynamics simulations and free energy calculations. Molecular BioSystems, 9(3), 361-374.
129. Bathini, R., Sivan, S. K., Fatima, S., & Manga, V. (2016). Molecular docking, MM/GBSA and 3D-QSAR studies on EGFR inhibitors. Journal of Chemical Sciences, 128(7), 1163-1173.
130. Pandey, R. K., Kumbhar, B. V., Sundar, S., Kunwar, A., & Prajapati, V. K. (2017). Structure-based virtual screening, molecular docking, ADMET and molecular simulations to develop benzoxaborole analogs as potential inhibitor against Leishmania donovani trypanothione reductase. Journal of receptors and signal transduction, 37(1), 60-70.
131. Lagarias, P., Barkan, K., Tzortzini, E., Stampelou, M., Vrontaki, E., Ladds, G., &Kolocouris, A. (2019). Insights to the binding of a selective adenosine A3 receptor antagonist using molecular dynamic simulations, MM-PBSA and MM-GBSA free energy calculations, and mutagenesis. Journal of chemical information and modeling, 59(12), 5183-5197.
132. Tang, X., Wang, Z., Lei, T., Zhou, W., Chang, S., & Li, D. (2018). Importance of protein flexibility on molecular recognition: modeling binding mechanisms of aminopyrazine inhibitors to Nek2. Physical Chemistry Chemical Physics, 20(8), 5591-5605.

133. Negron, C., Pearlman, D. A., & Del Angel, G. (2019). Predicting mutations deleterious to function in beta-lactamase TEM1 using MM-GBSA. Plos one, 14(3), e0214015.
134. Paissoni, C., Spiliotopoulos, D., Musco, G., &Spitaleri, A. (2015). GMXPBSA 2.1: A GROMACS tool to perform MM/PBSA and computational alanine scanning. Computer Physics Communications, 186, 105-107.
135. Salas-Burgos, A., Iserovich, P., Zuniga, F., Vera, J. C., &Fischbarg, J. (2004). Predicting the three-dimensional structure of the human facilitative glucose transporter glut1 by a novel evolutionary homology strategy: insights on the molecular mechanism of substrate migration, and binding sites for glucose and inhibitory molecules. Biophysical journal, 87(5), 2990-2999.
136. Shukla, R., Chetri, P. B., Sonkar, A., Pakharukova, M. Y., Mordvinov, V. A., & Tripathi, T. (2018). Identification of novel natural inhibitors of Opisthorchis felineus cytochrome P450 using structure-based screening and molecular dynamic simulation. Journal of Biomolecular Structure and Dynamics, 36(13), 3541-3556.
137. Verma, P., Tiwari, M., & Tiwari, V. (2018). In silico high-throughput virtual screening and molecular dynamics simulation study to identify inhibitor for AdeABC efflux pump of Acinetobacter baumannii. Journal of Biomolecular Structure and Dynamics, 36(5), 1182-1194.
138. Thirumal, K. D., Mendonca, E., Priyadharshini, C. J., George, P. D. C., & Zayed, H. (2019). A computational model to predict the structural and functional consequences of missense mutations in O6-methylguanine DNA methyltransferase. Advances in protein chemistry and structural biology, 115, 351.
139. Shukla, R., Shukla, H., Kalita, P., & Tripathi, T. (2018). Structural insights into natural compounds as inhibitors of Fasciola gigantica thioredoxin glutathione reductase. Journal of cellular biochemistry, 119(4), 3067-3080.
140. Kubarenko, A., Frank, M., & Weber, A. N. R. (2007). Structure–function relationships of Toll-like receptor domains through homology modelling and molecular dynamics. Biochemical Society Transactions, 35(6), 1515-1518.
141. Kumar, D. T., Mendonca, E., Christy, J. P., Doss, C. G. P., & Zayed, H. (2019). A computational model to predict the structural and functional consequences of missense mutations in O6-methylguanine DNA methyltransferase. Advances in Protein Chemistry and Structural Biology, 115, 351-369.
142. Baul, H. S., &Rajiniraja, M. (2018). Mechanistic study of the inhibition of monoamine oxidase-B by quercetin as the potential therapeutic strategy for Parkinson's Disease: An in silico approach. Journal of Computational Methods in Sciences and Engineering, 18(4), 1067-1073.
143. Di Prinzio, C. L., & Pereyra, R. G. (2016). Molecular dynamics simulations of tilt grain boundaries in ice. Modelling and Simulation in Materials Science and Engineering, 24(4), 045015.
144. Shah, M., Anwar, M. A., Yesudhas, D., Krishnan, J., & Choi, S. (2016). A structural insight into the negative effects of opioids in analgesia by modulating the TLR4 signaling: An in silico approach. Scientific reports, 6(1), 1-15.

145. Tian, J., Wang, P., Gao, S., Chu, X., Wu, N., & Fan, Y. (2010). Enhanced thermostability of methyl parathion hydrolase from Ochrobactrum sp. M231 by rational engineering of a glycine to proline mutation. The FEBS journal, 277(23), 4901-4908.
146. Joshi, T., Sharma, P., Joshi, T., & Chandra, S. (2020). In silico screening of anti-inflammatory compounds from Lichen by targeting cyclooxygenase-2. Journal of Biomolecular Structure and Dynamics, 38(12), 3544-3562.
147. Torktaz, I., Najafi, A., Golmohamadi, R., &Hassani, S. (2018). Molecular dynamics simulation (MDS) analysis of Vibrio cholerae ToxT virulence factor complexed with docked potential inhibitors. Bioinformation, 14(3), 101.
148. Raftopoulou, S., Nicolaides, N. C., Papageorgiou, L., Amfilochiou, A., Zakinthinos, S. G., George, P., &Vlachakis, D. (2020). Structural Study of the DNA: Clock/Bmal1 Complex Provides Insights for the Role of Cortisol, hGR, and HPA Axis in Stress Management and Sleep Disorders. In GeNeDis 2018 (pp. 59-71). Springer, Cham.
149. Muthuvel, S. K., & Elumalai, E. (2018). Molecular docking and dynamics studies of 4-anilino quinazolines for epidermal growth factor receptor tyrosine kinase to find potent inhibitor. Journal of Receptors and Signal Transduction, 38(5-6), 475-483.
150. Gajendrarao, P., Krishnamoorthy, N., Sakkiah, S., Lazar, P., & Lee, K. W. (2010). Molecular modeling study on orphan human protein CYP4A22 for identification of potential ligand binding site. Journal of Molecular Graphics and Modelling, 28(6), 524-532.
151. Tanwar, H., Kumar, D. T., Doss, C. G. P., & Zayed, H. (2019). Bioinformatics classification of mutations in patients with Mucopolysaccharidosis IIIA. Metabolic brain disease, 34(6), 1577-1594.
152. Kumari, R., Kumar, R., Open Source Drug Discovery Consortium, & Lynn, A. (2014). g_mmpbsa□ A GROMACS tool for high-throughput MM-PBSA calculations. Journal of chemical information and modeling, 54(7), 1951-1962.
153. Paissoni, C., Spiliotopoulos, D., Musco, G., &Spitaleri, A. (2014). GMXPBSA 2.0: A GROMACS tool to perform MM/PBSA and computational alanine scanning. Computer Physics Communications, 185(11), 2920-2929.
154. Wang, E., Sun, H., Wang, J., Wang, Z., Liu, H., Zhang, J. Z., & Hou, T. (2019). End-point binding free energy calculation with MM/PBSA and MM/GBSA: strategies and applications in drug design. Chemical reviews, 119(16), 9478-9508.
155. Kumar, A., Srivastava, G., Negi, A. S., & Sharma, A. (2019). Docking, molecular dynamics, binding energy-MM-PBSA studies of naphthofuran derivatives to identify potential dual inhibitors against BACE-1 and GSK-3β. Journal of Biomolecular Structure and Dynamics, 37(2), 275-290.
156. Botelho, F. D., Dos Santos, M. C., Gonçalves, A. D. S., Kuca, K., Valis, M., LaPlante, S. R., & de Almeida, J. S. (2020). Ligand-based virtual screening, molecular docking, molecular dynamics, and MM-PBSA calculations towards the identification of potential novel ricin inhibitors. Toxins, 12(12), 746.
157. Elkarhat, Z., Charoute, H., Elkhattabi, L., Barakat, A., &Rouba, H. (2020). Potential inhibitors of SARS-cov-2 RNA dependent RNA polymerase protein: molecular docking, molecular dynamics simulations

and MM-PBSA analyses. Journal of Biomolecular Structure and Dynamics, 1-14.

158. Martins, L. C., Torres, P. H. M., de Oliveira, R. B., Pascutti, P. G., Cino, E. A., & Ferreira, R. S. (2018). Investigation of the binding mode of a novel cruzain inhibitor by docking, molecular dynamics, ab initio and MM/PBSA calculations. Journal of computer-aided molecular design, 32(5), 591-605.
159. Kumari, R., & Lynn, A. (2011). Application of MM/PBSA in the prediction of relative binding free energy: Re-scoring of docking hit-list. Journal of Natural Science, Biology and Medicine, 2(3), 92-92.
160. Shenai, P. M., Xu, Z., & Zhao, Y. (2012). Applications of principal component analysis (PCA) in materials science. Principal component analysis–engineering applications, 25-40.
161. Chen, J., Wang, J., & Zhu, W. (2016). Molecular mechanism and energy basis of conformational diversity of antibody SPE7 revealed by molecular dynamics simulation and principal component analysis. Scientific reports, 6(1), 1-12.
162. Sittel, F., Filk, T., & Stock, G. (2017). Principal component analysis on a torus: Theory and application to protein dynamics. The Journal of chemical physics, 147(24), 244101.
163. Riccardi, L., Nguyen, P. H., & Stock, G. (2009). Free-energy landscape of RNA hairpins constructed via dihedral angle principal component analysis. The Journal of Physical Chemistry B, 113(52), 16660-16668.
164. Buslaev, P., Mustafin, K., &Gushchin, I. (2020). Principal component analysis highlights the influence of temperature, curvature and cholesterol on conformational dynamics of lipids. Biochimica et Biophysica Acta (BBA)-Biomembranes, 1862(7), 183253.
165. Nguyen, P. H. (2006). Complexity of free energy landscapes of peptides revealed by nonlinear principal component analysis. Proteins: Structure, Function, and Bioinformatics, 65(4), 898-913.
166. Yamamoto, N. (2014). Hot spot of structural ambivalence in prion protein revealed by secondary structure principal component analysis. The Journal of Physical Chemistry B, 118(33), 9826-9833.
167. Michielssens, S., van Erp, T. S., Kutzner, C., Ceulemans, A., & de Groot, B. L. (2012). Molecular dynamics in principal component space. The Journal of Physical Chemistry B, 116(29), 8350-8354.
168. Grasso, G., Deriu, M. A., Tuszynski, J. A., Gallo, D., Morbiducci, U., &Danani, A. (2016). Conformational fluctuations of the AXH monomer of Ataxin-1. Proteins: Structure, Function, and Bioinformatics, 84(1), 52-59.
169. Verma, S., Singh, A., Kumari, A., Tyagi, C., Goyal, S., Jamal, S., & Grover, A. (2017). Natural polyphenolic inhibitors against the antiapoptotic BCL-2. Journal of Receptors and Signal Transduction, 37(4), 391-400.
170. Mouritsen, O. G., &Khandelia, H. (2012). Molecular mechanism of the allosteric enhancement of the umami taste sensation. The FEBS journal, 279(17), 3112-3120.
171. Swain, S. S., Paidesetty, S. K., Dehury, B., Sahoo, J., Vedithi, S. C., Mahapatra, N., &Padhy, R. N. (2018). Molecular docking and simulation study for synthesis of alternative dapsone derivative as a newer antileprosy drug in multidrug therapy. Journal of cellular biochemistry, 119(12), 9838-9852.

172. Villa, A., & Stock, G. (2006). What NMR relaxation can tell us about the internal motion of an RNA hairpin: a molecular dynamics simulation study. Journal of chemical theory and computation, 2(5), 1228-1236.
173. Ng, H. W., Laughton, C. A., & Doughty, S. W. (2013). Molecular dynamics simulations of the adenosine A2a receptor: structural stability, sampling, and convergence. Journal of chemical information and modeling, 53(5), 1168-1178.

Figures

Figure 1

Protein 3D structure of VEGF (PDBID: 3V2A) obtained from PDB database

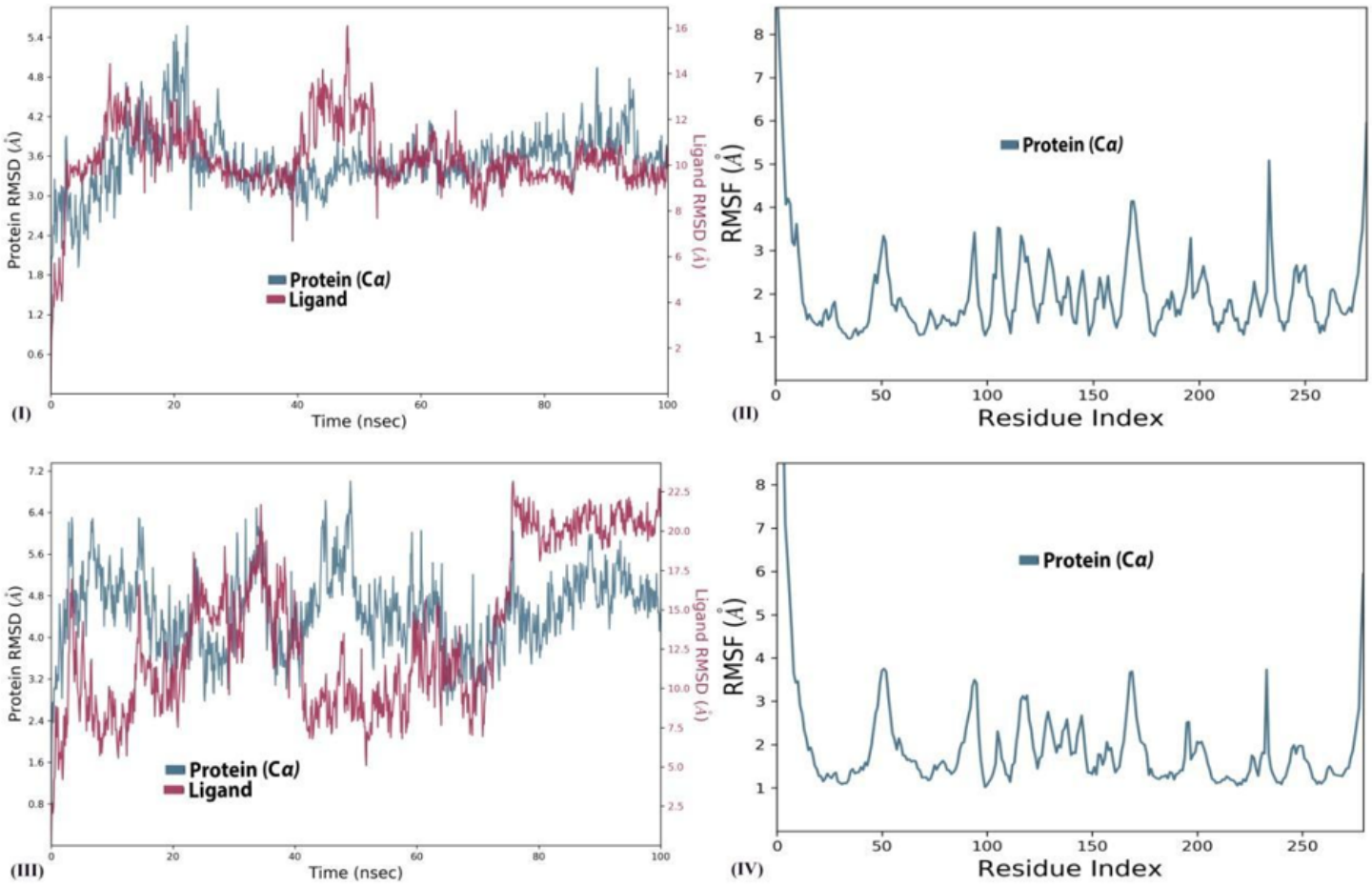

Figure 2

Molecular dynamics RMSD and RMSF of free VEGF (I,II); VEGFR complex with best established compound (PubChem CID: 10297043) (III,IV); VEGF complex with the best virtual screened compound (PubChem CID: 88265020)

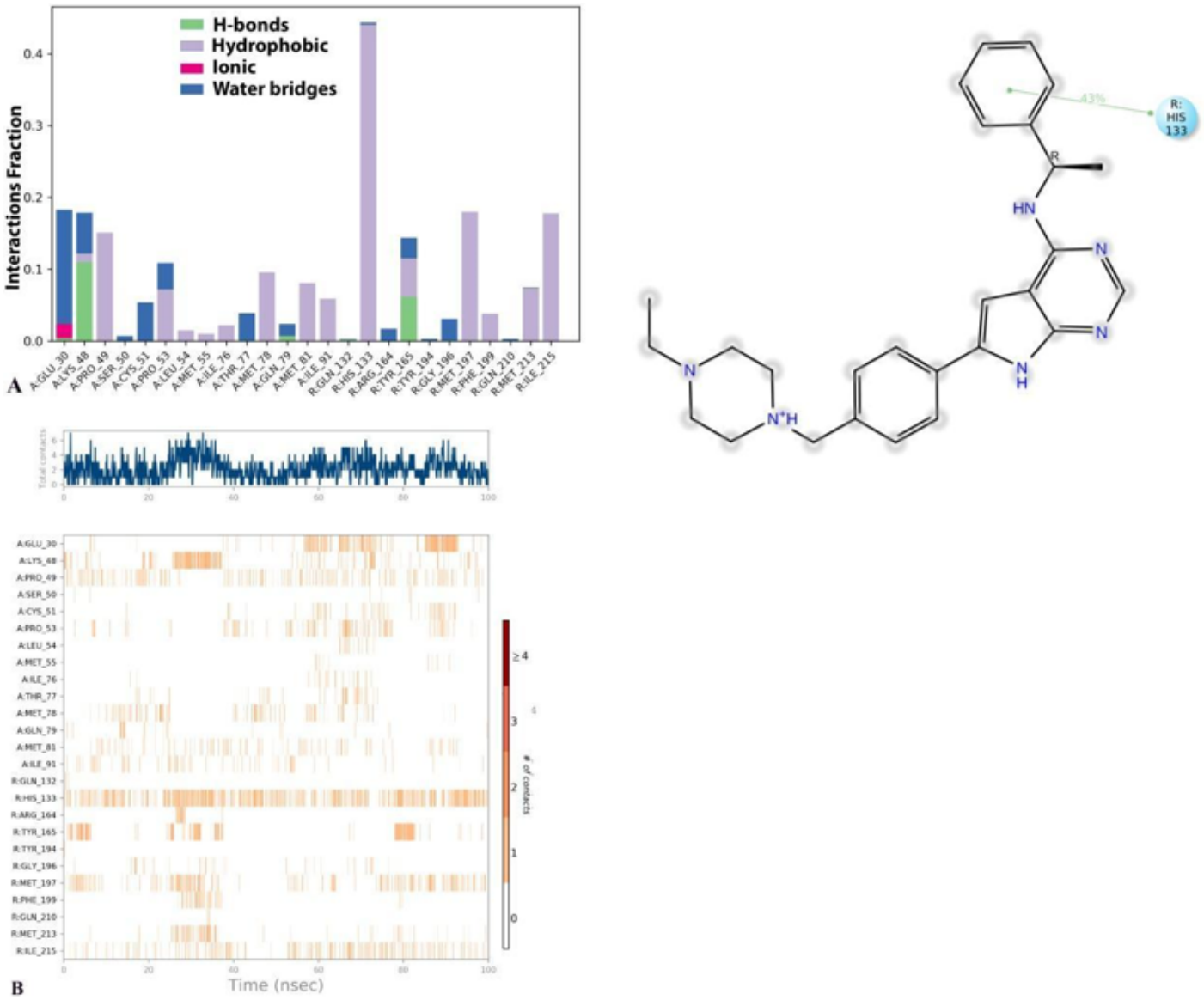

Figure 3

Interaction diagram of VEGF complex with best established compound PubChem CID: 10297043 observed during the molecular dynamics simulation. (A) The protein-ligand interaction diagram. (B) The residues that interact with the ligand in each trajectory frame. (C) Schematic diagram of ligand interaction with the amino acid residues of protein during MD simulation.

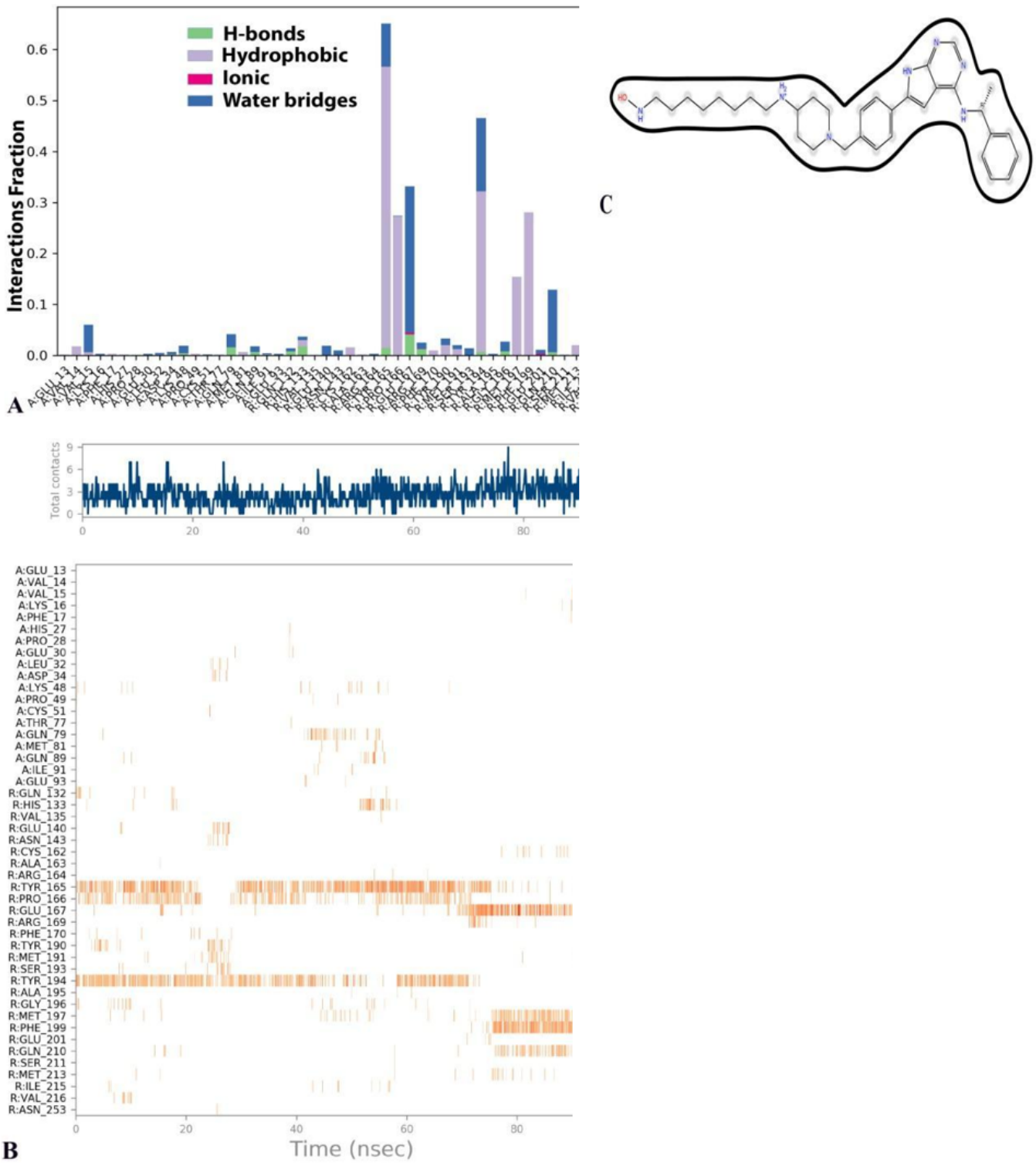

Figure 4

Interaction diagram of VEGF complex with best virtually screened compound (PubChem CID: 88265020) observed during the molecular dynamics simulation. (A) The protein-ligand interaction diagram. (B) The residues that interact with the ligand in each trajectory frame. (C) Schematic diagram of ligand interaction with the amino acid residues of protein during MD simulation.

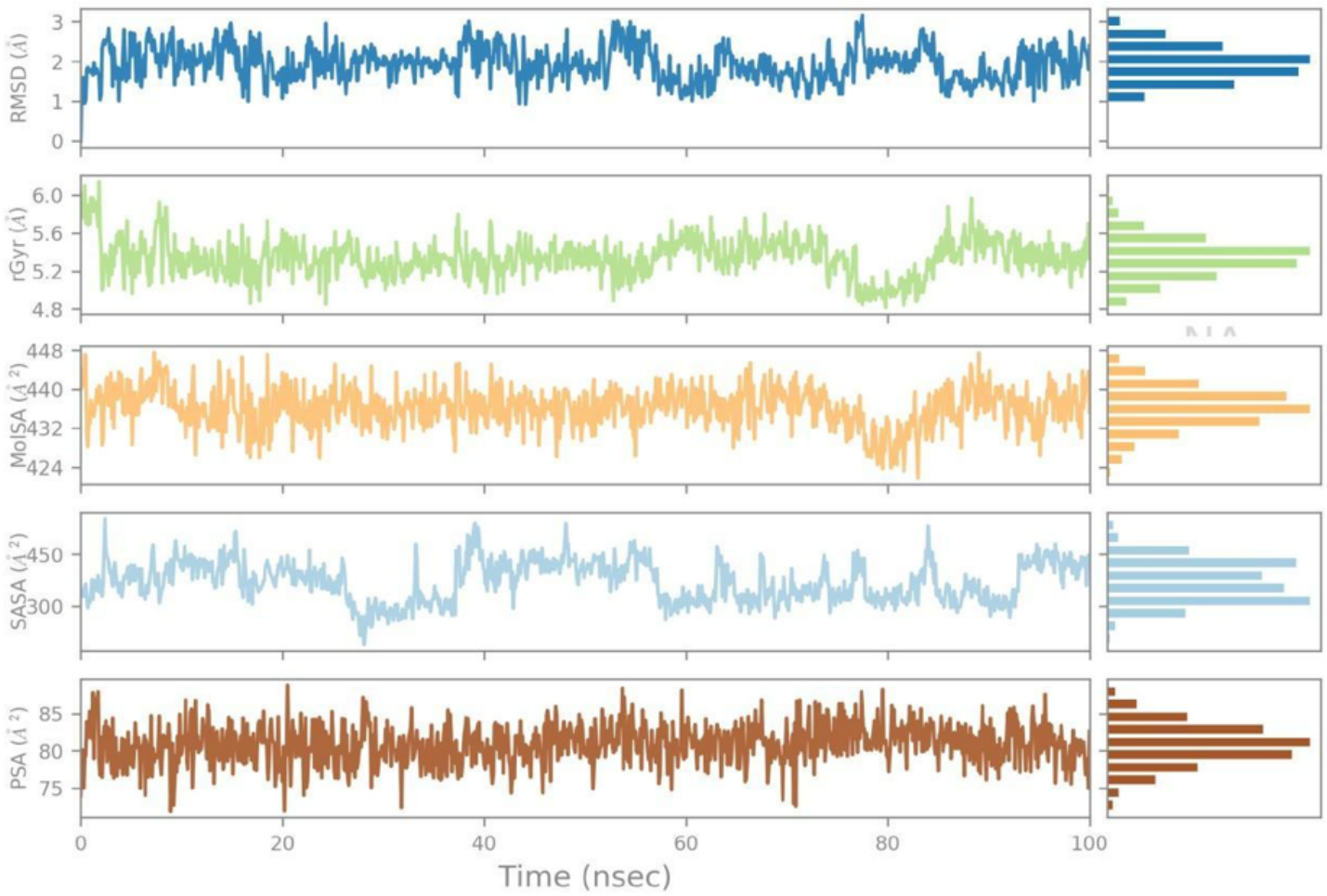

Figure 5

The ligand property trajectory of the VEGF complex with best established compound PubChem CID: 10297043during the 100 ns simulation.

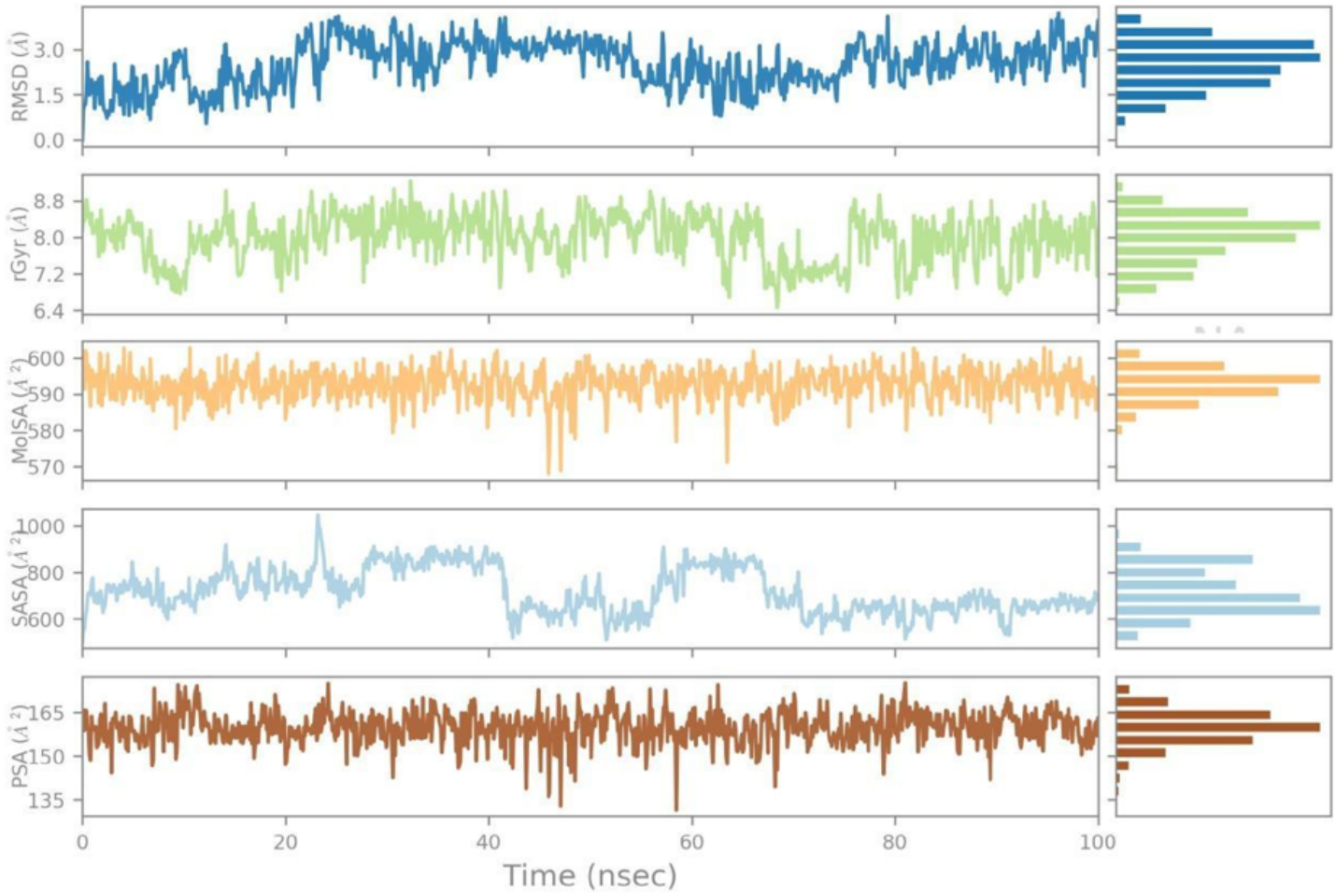

Figure 6

The ligand property trajectory of the VEGF complex with best virtually screened compound PubChem CID: 88265020 during the 100 ns simulation.

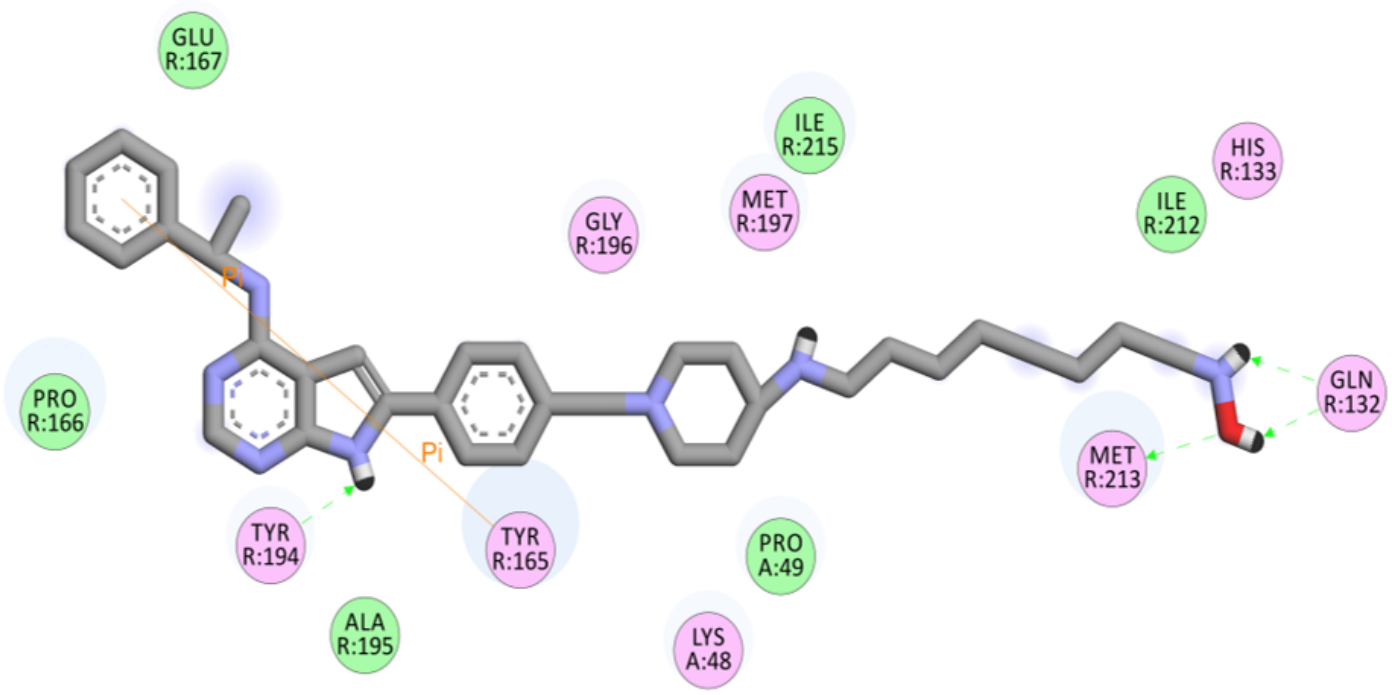

Figure 7

The most effective Virtual Screened compound (PubChem ID: 88265020), binding with VEGF shows Van der Waals interaction

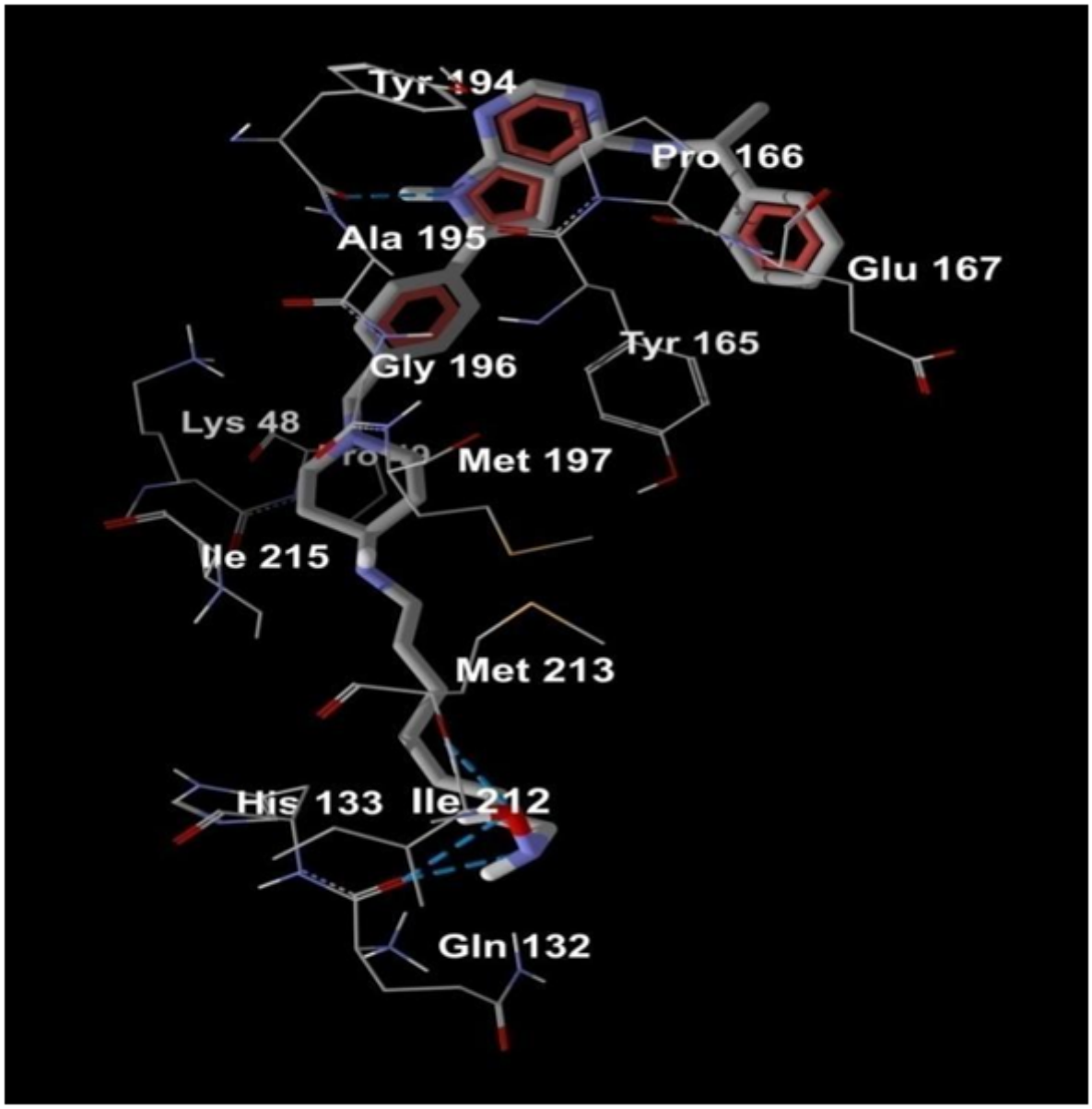

Figure 8

The most effective Virtual screened compound (PubChem ID: 88265020), binding with VEGF shows Hydrogen Bond interaction

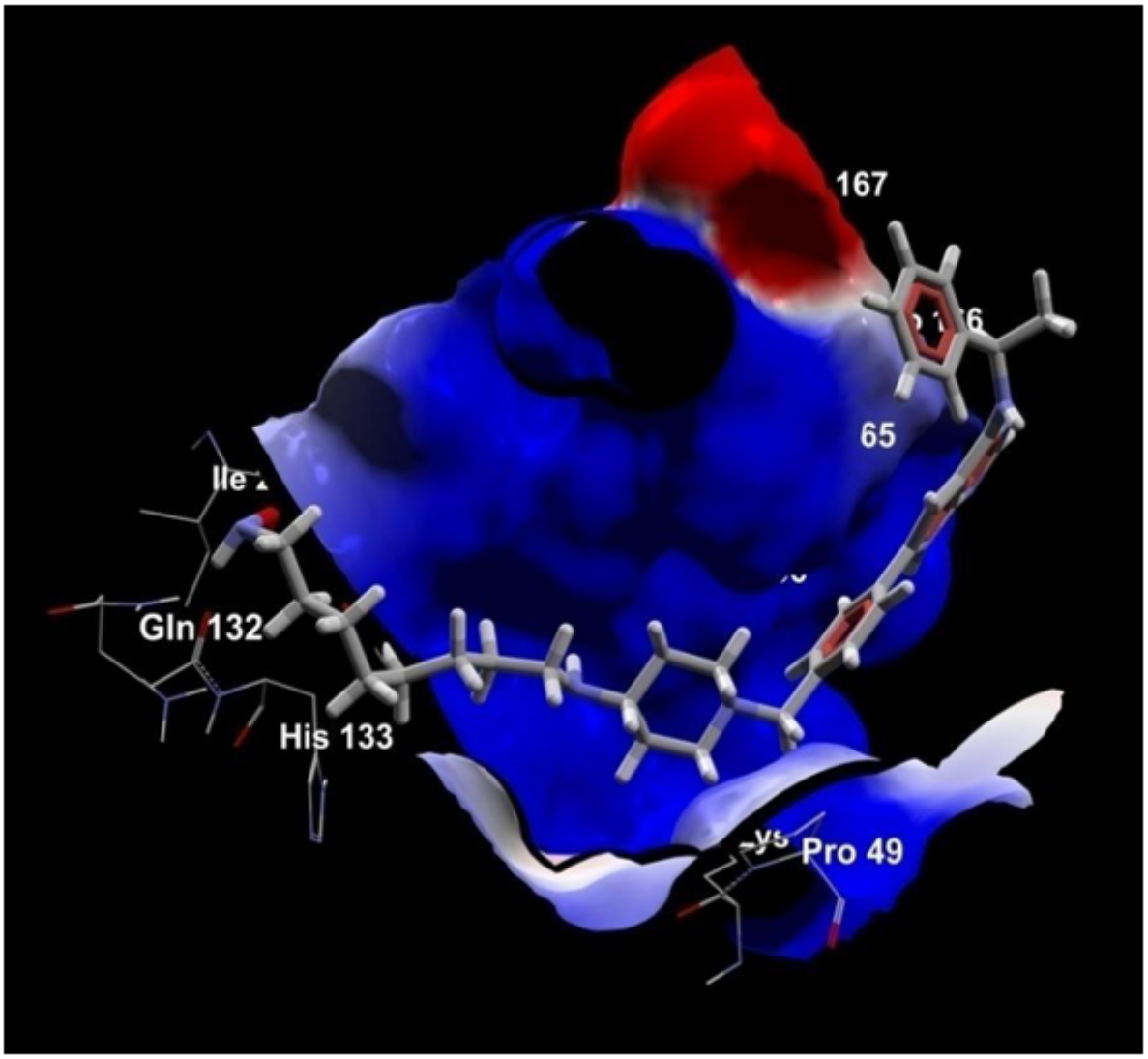

Figure 9

The most effective Virtual Screened compound (Pubchem ID: 88265020), binding with VEGF shows Electrostatic interaction

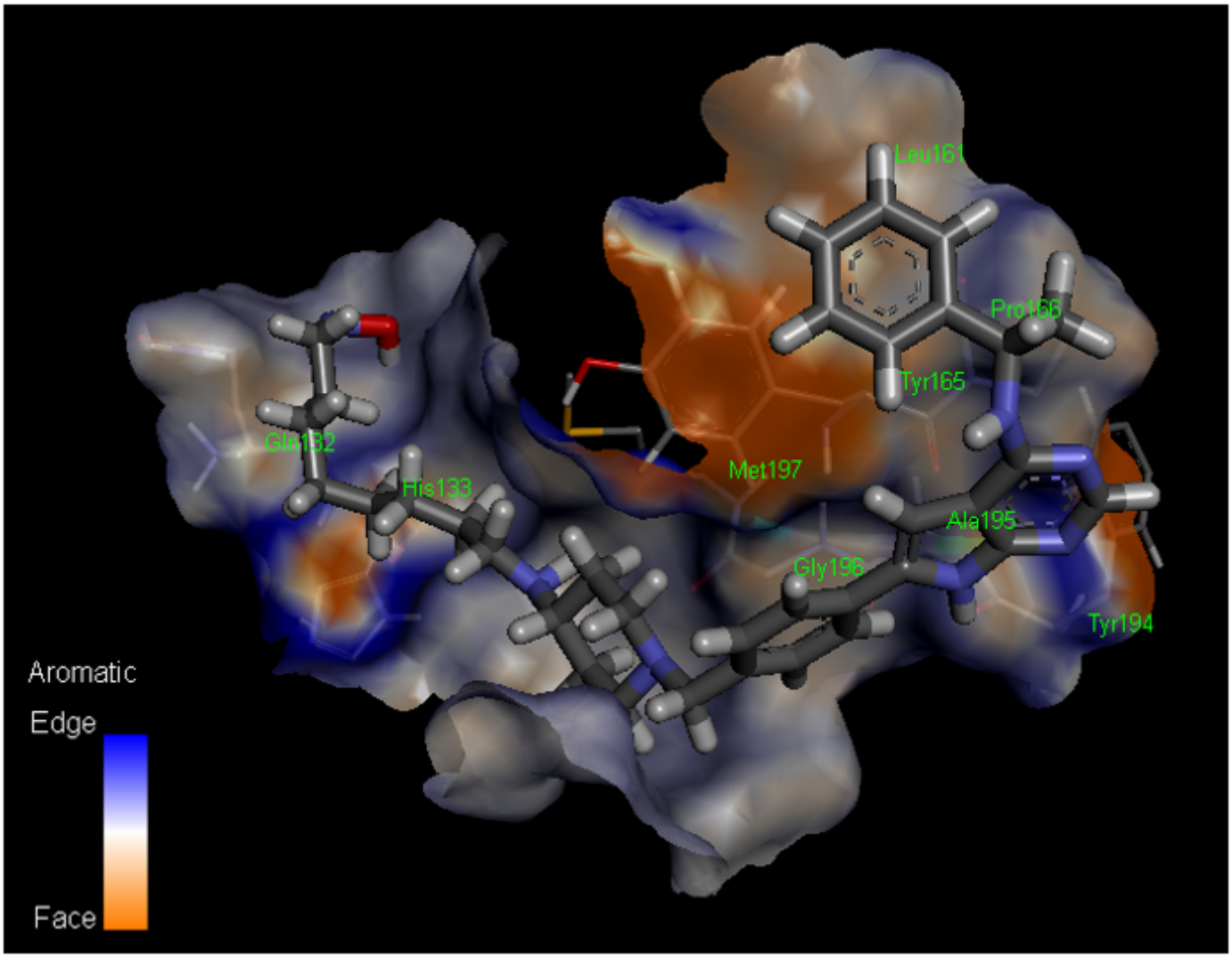

Figure 10

The most effective Virtual Screened compound (Pubchem ID: 88265020), binding with VEGF shows aromatic interaction

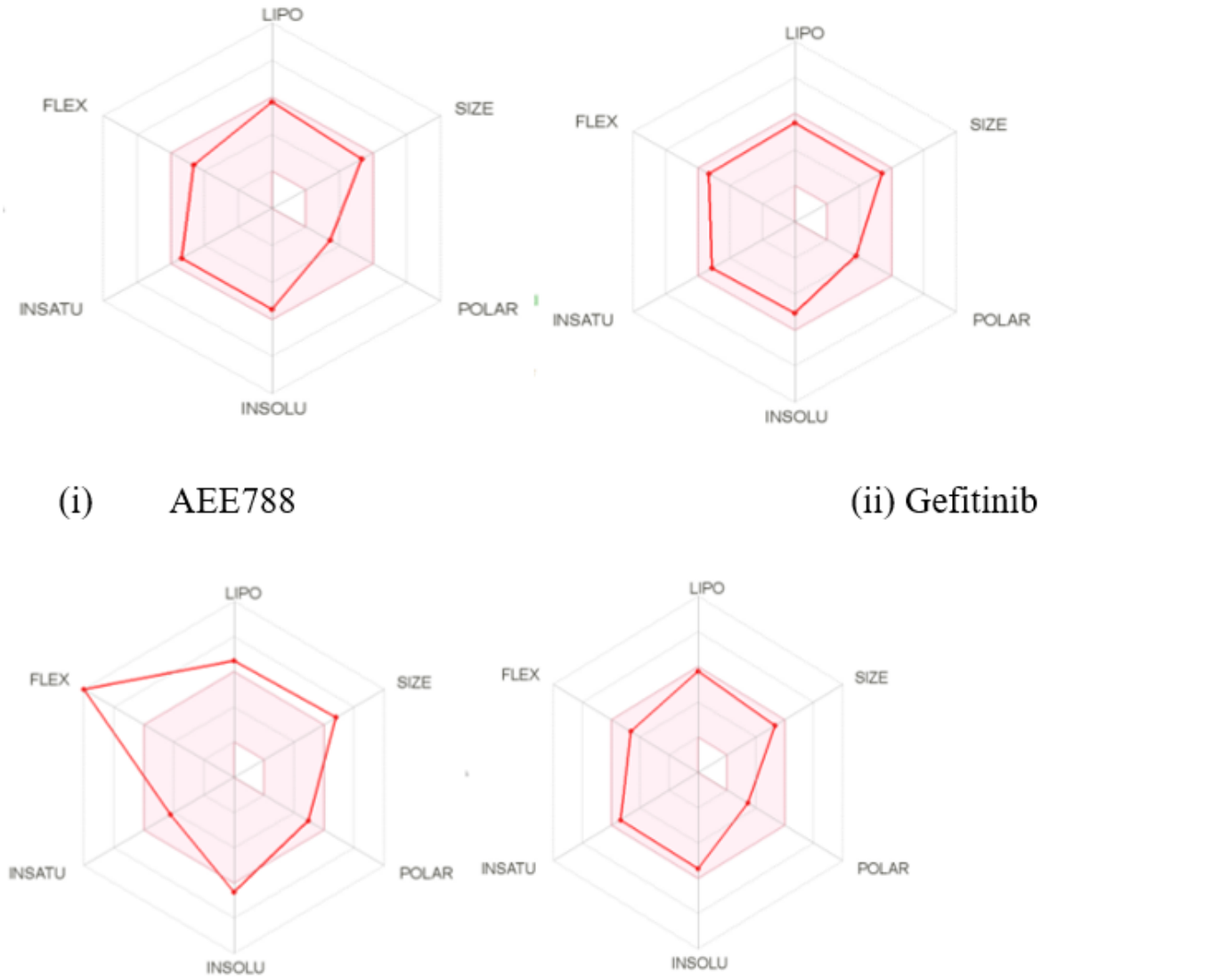

Figure 11

Bioavailability radar related to physicochemical properties of two of each best compounds from established docked result and virtually screened result

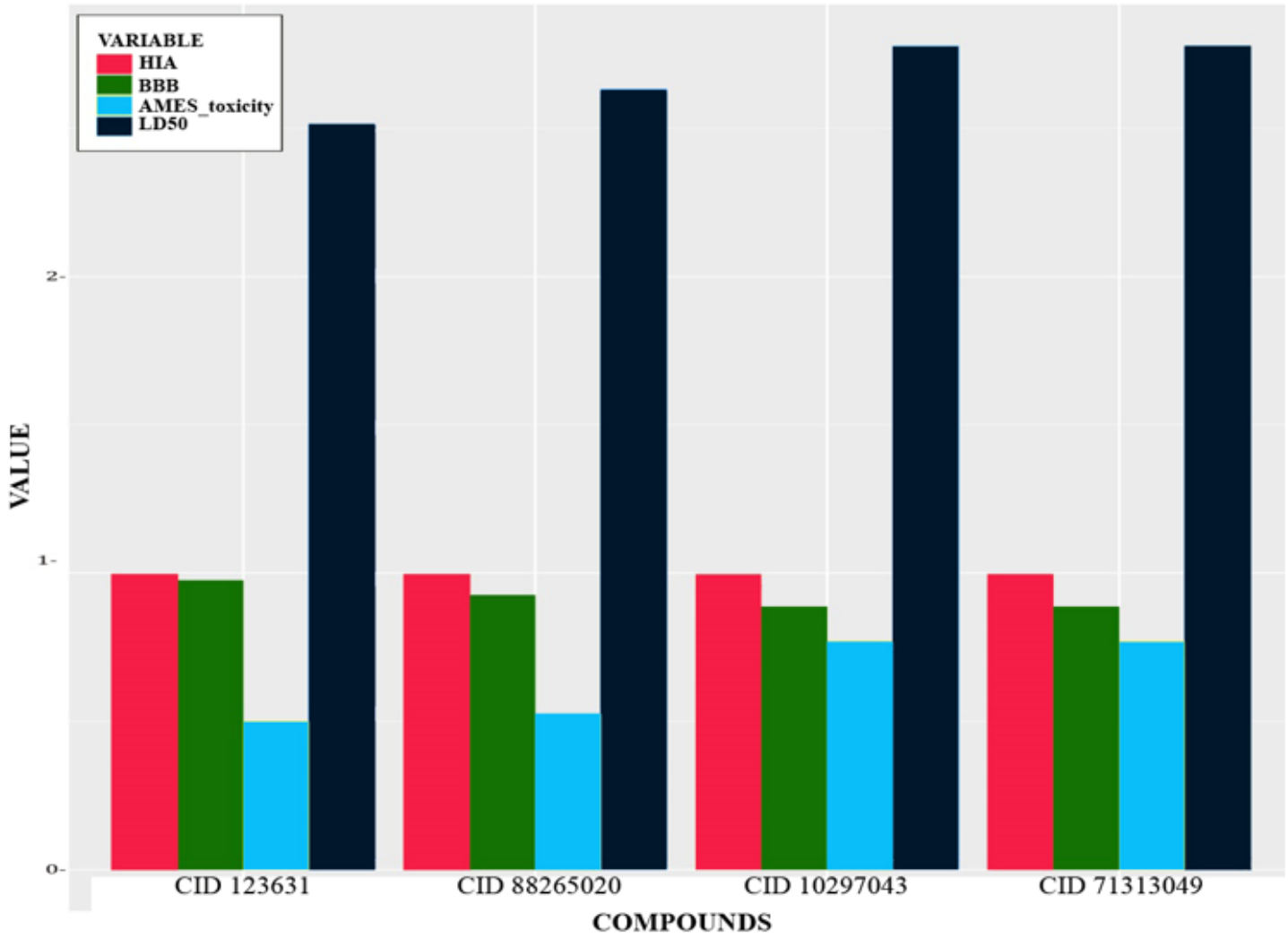

Figure 12

Comparative HIA, BBB, AMES toxicity, LD50 of the Established compounds against Virtual screened compounds

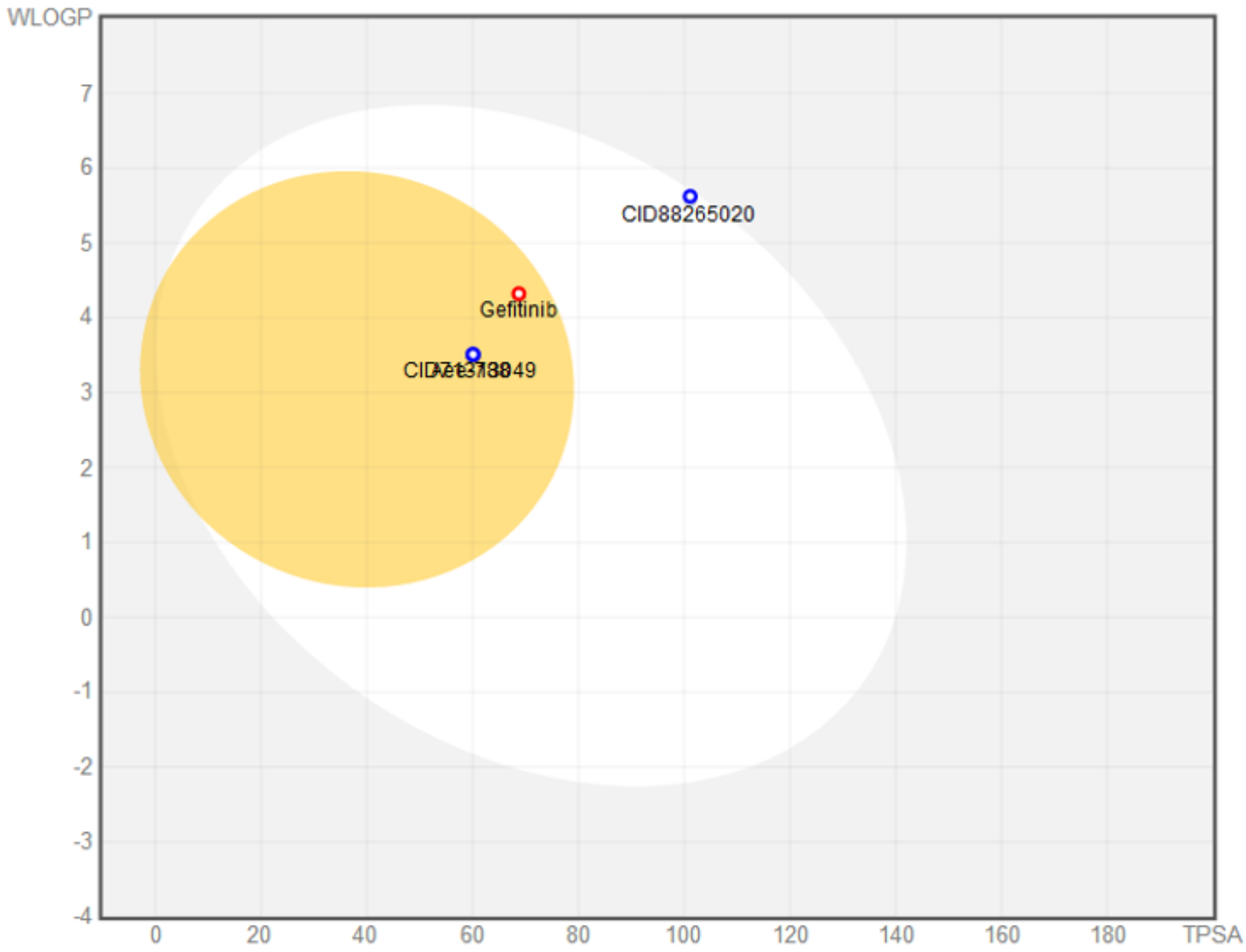

Figure 13

Boiled Egg Plot of 4 most effective Virtual Screened and Established drugs.